

# Accurate Implicit–Explicit General Linear Methods with Inherent Runge–Kutta Stability

Michał Braś<sup>1</sup> · Giuseppe Izzo<sup>2</sup>  ·  
Zdzisław Jackiewicz<sup>1,3</sup>

Received: 16 December 2015 / Revised: 19 April 2016 / Accepted: 22 August 2016 /  
Published online: 1 September 2016  
© Springer Science+Business Media New York 2016

**Abstract** We investigate implicit–explicit (IMEX) general linear methods (GLMs) with inherent Runge–Kutta stability (IRKS) for differential systems with non-stiff and stiff processes. The construction of such formulas starts with implicit GLMs with IRKS which are  $A$ - and  $L$ -stable, and then we ‘remove’ implicitness in non-stiff terms by extrapolating unknown stage derivatives by stage derivatives which are already computed by the method. Then we search for IMEX schemes with large regions of absolute stability of the ‘explicit part’ of the method assuming that the ‘implicit part’ of the scheme is  $A(\alpha)$ -stable for some  $\alpha \in (0, \pi/2]$ . Examples of highly stable IMEX GLMs are provided of order  $1 \leq p \leq 4$ . Numerical examples are also given which illustrate good performance of these schemes.

**Keywords** IMEX methods · General linear methods · Inherent Runge–Kutta stability · Convergence and stability analysis · Construction of highly stable methods

---

The work of Michał Braś was supported by the National Science Center under Grant DEC-2011/01/N/ST1/02672 and the Polish Ministry of Science and Higher Education. The work of Giuseppe Izzo was partially supported by GNCS-INdAM.

---

✉ Giuseppe Izzo  
giuseppe.izzo@unina.it

Michał Braś  
bras@agh.edu.pl

Zdzisław Jackiewicz  
jackiewicz@asu.edu

<sup>1</sup> Faculty of Applied Mathematics, AGH University of Science and Technology, Kraków, Poland

<sup>2</sup> Dipartimento di Matematica e Applicazioni, Università di Napoli-“Federico II”, 80126 Naples, Italy

<sup>3</sup> School of Mathematical and Statistical Sciences, Arizona State University, Tempe, AZ 85287, USA

### 1 Introduction

Consider the initial value problem for the system of ordinary differential equations (ODEs) of the form

$$\begin{cases} y'(t) = f(y(t)) + g(y(t)), & t \in [t_0, T], \\ y(t_0) = y_0 \in \mathbb{R}^m, \end{cases} \tag{1.1}$$

where  $f : \mathbb{R}^m \rightarrow \mathbb{R}^m$  represents the non-stiff processes, and  $g : \mathbb{R}^m \rightarrow \mathbb{R}^m$  represents stiff processes. Such systems arise in many practical applications in science and engineering, for example in semidiscretization of time-dependent advection-diffusion-reaction partial differential equations (PDEs), where  $f(y)$  represents the semidiscretization in space variables of advection terms, and  $g(y)$  represents the semidiscretization in space variables of diffusion or chemical reaction terms, compare [29].

For efficient integration of such systems we will consider the class of implicit–explicit (IMEX) methods, where the non-stiff part  $f(y)$  of (1.1) is integrated by explicit numerical scheme, and stiff part  $g(y)$  of (1.1) is integrated by implicit numerical method. In this paper we will investigate the class of IMEX general linear methods (GLMs) with inherent Runge–Kutta stability (IRKS). For these formulas the stability matrix has only one nonzero eigenvalue, which is an approximation of order  $p$  to the exponential function  $\exp(z)$ . As a consequence, the stability behavior of such methods is similar to that of Runge–Kutta formulas of the same order.

We will start with diagonally implicit GLMs for (1.1) of the form

$$\begin{cases} Y_i^{[n+1]} = h \sum_{j=1}^i a_{ij} \left( f \left( Y_j^{[n+1]} \right) + g \left( Y_j^{[n+1]} \right) \right) + \sum_{j=1}^r u_{ij} y_j^{[n]}, & i = 1, 2, \dots, s, \\ y_i^{[n+1]} = h \sum_{j=1}^s b_{ij} \left( f \left( Y_j^{[n+1]} \right) + g \left( Y_j^{[n+1]} \right) \right) + \sum_{j=1}^r v_{ij} y_j^{[n]}, & i = 1, 2, \dots, r, \end{cases} \tag{1.2}$$

$n = 0, 1, \dots, N - 1, h = (T - t_0)/N$ , with some desirable accuracy and linear stability properties. GLMs will be reviewed in Sect. 2, GLMs with RK and IRKS properties will be discussed in Sect. 3, and the algorithm for construction of GLMs with IRKS properties is then described in Sect. 4. Then we will ‘remove’ the implicitness in non-stiff terms by extrapolating  $f(Y_j^{[n+1]})$  by linear combinations of  $f(Y_k^{[n]})$ ,  $k = 1, 2, \dots, s$ , and  $f(Y_k^{[n+1]})$ ,  $k = 1, 2, \dots, j - 1$ , which are already known. This extrapolation-based approach was first proposed by Cardone et al. [20,21] (see also the report [19] for more details) in the context of diagonally implicit multistage integration methods (DIMSIMs) and Runge–Kutta (RK) methods, and it will be applied in Sect. 5 to the class of GLMs with IRKS. Convergence and error analysis of IMEX GLMs with IRKS is presented in Sect. 6. Linear stability analysis of IMEX GLMs with respect to the test equation with linear terms corresponding to non-stiff and stiff parts of (1.1) is presented in Sect. 7. Construction of IMEX methods with large regions of absolute stability of the ‘explicit part’ of the method, assuming that the ‘implicit part’ of the method is  $A(\alpha)$ -stable for  $0 < \alpha \leq \pi/2$ , is described in Sect. 8. Examples of such methods are given in Sects. 8.1–8.4 for  $p = q$  up to four, and  $r = s = p + 1$  up to five. Here,  $p$  is the order,  $q$  is the stage order,  $r$  is the number of external approximations and  $s$  is the number of internal approximations in (1.2). The results of some numerical experiments with IMEX GLMs with IRKS are presented in Sect. 9. Concluding remarks and plans for future work are described in Sect. 10.

## 2 A Short Introduction to GLMs

In this section we review GLMs with IRKS. Consider the initial-value problem for the system of ODEs

$$\begin{cases} y'(t) = F(y(t)), & t \in [t_0, T], \\ y(t_0) = y_0 \in \mathbb{R}^m, \end{cases} \tag{2.1}$$

where the function  $F : \mathbb{R}^m \rightarrow \mathbb{R}^m$  is assumed to be sufficiently smooth. Let  $N$  be a positive integer and define the stepsize  $h = (T - t_0)/N$ . On the uniform grid  $t_0 < t_1 < \dots < t_N = T$ ,  $t_n = t_0 + nh$ ,  $n = 0, 1, \dots, N$ , the GLMs for (2.1) are defined by

$$\begin{cases} Y_i^{[n+1]} = h \sum_{j=1}^i a_{ij} F(Y_j^{[n+1]}) + \sum_{j=1}^r u_{ij} y_j^{[n]}, & i = 1, 2, \dots, s, \\ y_i^{[n+1]} = h \sum_{j=1}^s b_{ij} F(Y_j^{[n+1]}) + \sum_{j=1}^r v_{ij} y_j^{[n]}, & i = 1, 2, \dots, r, \end{cases} \tag{2.2}$$

$n = 0, 1, \dots, N - 1$ , compare [12, 13, 26, 27, 33]. Here, the quantities  $Y_i^{[n+1]}$  are approximations of stage order  $q$  to the solution  $y$  of (2.1) at the points  $t_n + c_i h$ , i.e.,

$$Y_i^{[n+1]} = y(t_n + c_i h) + O(h^{q+1}), \quad i = 1, 2, \dots, s, \tag{2.3}$$

and  $y_i^{[n]}$  are approximations of order  $p$  to the linear combinations of scaled derivatives of  $y$  at the point  $t_n$ , i.e.,

$$y_i^{[n]} = \sum_{k=0}^p q_{ik} h^k y^{(k)}(t_n) + O(h^{p+1}), \quad i = 1, 2, \dots, r. \tag{2.4}$$

The GLMs (2.2) are characterized by the abscissa vector  $\mathbf{c} = [c_1, c_2, \dots, c_s]^T$ , four coefficient matrices  $\mathbf{A} = [a_{ij}]$ ,  $\mathbf{U} = [u_{ij}]$ ,  $\mathbf{B} = [b_{ij}]$ ,  $\mathbf{V} = [v_{ij}]$ , where  $\mathbf{A} \in \mathbb{R}^{s \times s}$ ,  $\mathbf{U} \in \mathbb{R}^{s \times r}$ ,  $\mathbf{B} \in \mathbb{R}^{r \times s}$ ,  $\mathbf{V} \in \mathbb{R}^{r \times r}$ , the vectors  $\mathbf{q}_k = [q_{1,k}, q_{2,k}, \dots, q_{r,k}]^T$ ,  $k = 0, 1, \dots, p$ , appearing in (2.4), and the four integers: the order of the method  $p$  [compare (2.4)], the stage order  $q$  [compare (2.3)], the number of external approximations  $r$ , and the number of internal approximations or stages  $s$ .

In what follows we consider the class of GLMs (2.2) such that  $p = q$  and  $r = s = p + 1$ . We will also assume that the coefficient matrix  $\mathbf{A}$  is lower triangular with the same element  $\lambda > 0$  on the diagonal. Denote by  $\mathbf{y}^{[n]}$  and  $\mathbf{y}^{[n+1]}$  vectors of dimension  $mr$  with vector components  $y_i^{[n]}$  and  $y_i^{[n+1]}$ ,  $i = 1, 2, \dots, r$ , of dimension  $m$ . We will assume that  $\mathbf{y}^{[n]}$  and  $\mathbf{y}^{[n+1]}$  are approximations of order  $q = p$  to the vectors  $\mathbf{z}(t_n, h)$  and  $\mathbf{z}(t_{n+1}, h)$ , where the so-called Nordsieck vector  $\mathbf{z}(t, h)$  is defined by

$$\mathbf{z}(t, h) = \begin{bmatrix} z_1(t, h) \\ z_2(t, h) \\ \vdots \\ z_s(t, h) \end{bmatrix} = \begin{bmatrix} y(t) \\ hy'(t) \\ \vdots \\ h^p y^{(p)}(t) \end{bmatrix} \in \mathbb{R}^{m \times (p+1)}. \tag{2.5}$$

It can be demonstrated (compare [31–33, 46]) that the method (2.2) has stage order  $q = p$  and order  $p$  if and only if

$$e^{cz} = z\mathbf{A}e^{cz} + \mathbf{UZ} + O(z^{p+1}), \tag{2.6}$$

and

$$e^z \mathbf{Z} = z\mathbf{B}e^{cz} + \mathbf{VZ} + O(z^{p+1}), \tag{2.7}$$

where the vector  $\mathbf{Z}$  is defined by  $\mathbf{Z} = [1, z, \dots, z^p]^T$ . In particular, comparing to zero constant terms in (2.6) and (2.7) we obtain the so-called preconistency conditions

$$\mathbf{U}\mathbf{e}_1 = \mathbf{e}, \quad \mathbf{V}\mathbf{e}_1 = \mathbf{e}_1, \tag{2.8}$$

where  $\mathbf{e}_1 = [1, 0, \dots, 0]^T \in \mathbb{R}^s$  and  $\mathbf{e} = [1, 1, \dots, 1]^T \in \mathbb{R}^s$ .

### 3 GLMs with RK and IRKS Properties

In this section we will review stability properties of GLMs (2.2) with respect to the linear test equation

$$y' = \xi y, \quad t \geq 0, \tag{3.1}$$

where  $\xi \in \mathbb{C}$ . Applying (2.2) to (3.1) we obtain the vector recurrence relation  $\mathbf{y}^{[n+1]} = \mathbf{M}(z)\mathbf{y}^{[n]}$ ,  $n = 1, 2, \dots$ ,  $z = h\xi$ , where the stability matrix  $\mathbf{M}(z)$  is defined by

$$\mathbf{M}(z) = \mathbf{V} + z\mathbf{B}(\mathbf{I} - z\mathbf{A})^{-1}\mathbf{U}, \tag{3.2}$$

and  $\mathbf{I}$  is the identity matrix of dimension  $s$ . We also define the stability function  $p(w, z)$  of (2.2) by the formula

$$p(w, z) = \det(w\mathbf{I} - \mathbf{M}(z)), \tag{3.3}$$

where  $\mathbf{I}$  is now the identity matrix of dimension  $r$ . The GLM (2.2) is said to have RK stability if  $p(w, z)$  has only one nonzero root, i.e., if

$$p(w, z) = w^{r-1}(w - R(z)), \tag{3.4}$$

where  $R(z)$  is the stability function of RK method of the same order.

Following [17,46] we say that two matrices  $\mathbf{A}$  and  $\mathbf{B}$  are equivalent, written as  $\mathbf{A} \equiv \mathbf{B}$ , if and only if they are identical except possibly their first rows. This equivalence relation plays an important role in the definition of IRKS. The GLM (2.2) with  $r = s$  satisfying preconistency conditions  $\mathbf{U}\mathbf{e}_1 = \mathbf{e}$  and  $\mathbf{V}\mathbf{e}_1 = \mathbf{e}_1$  is said to have IRKS property if there exists some matrix  $\mathbf{X}$  such that

$$\mathbf{B}\mathbf{A} \equiv \mathbf{X}\mathbf{B}, \tag{3.5}$$

$$\mathbf{B}\mathbf{U} \equiv \mathbf{X}\mathbf{V} - \mathbf{V}\mathbf{X}, \tag{3.6}$$

and

$$\det(w\mathbf{I} - \mathbf{V}) = w^p(w - 1). \tag{3.7}$$

The importance of these relations follows from the theorem proved by Butcher and Wright [17,46] that if the GLM (2.2) has IRKS property, i.e., if the relations (3.5), (3.6), and (3.7) hold, then GLM (2.2) has RK stability, i.e., its stability function  $p(w, z)$  satisfies (3.4). It was also proved in [17,46] that the stability function  $R(z)$  appearing in (3.4) can be computed from the formula

$$R(z) = \mathbf{e}_1^T(\mathbf{I} - z\mathbf{X})\mathbf{M}(z)(\mathbf{I} - z\mathbf{X})^{-1}\mathbf{e}_1.$$

Moreover, for GLMs (2.2) with  $p = q$  and  $r = s = p + 1$  the matrix  $\mathbf{X}$  appearing in (3.5) and (3.6) is a doubly companion matrix of the form

$$\mathbf{X} = \begin{bmatrix} -\alpha_1 & -\alpha_2 & -\alpha_3 & \cdots & -\alpha_{p-1} & -\alpha_p & -\alpha_{p+1} - \beta_{p+1} \\ 1 & 0 & 0 & \cdots & 0 & 0 & -\beta_p \\ 0 & 1 & 0 & \cdots & 0 & 0 & -\beta_{p-1} \\ \vdots & \vdots & \vdots & \ddots & \vdots & \vdots & \vdots \\ 0 & 0 & 0 & \cdots & 0 & 0 & -\beta_3 \\ 0 & 0 & 0 & \cdots & 1 & 0 & -\beta_2 \\ 0 & 0 & 0 & \cdots & 0 & 1 & -\beta_1 \end{bmatrix}, \tag{3.8}$$

which depends on free parameters  $\alpha_i$  and  $\beta_i, i = 1, 2, \dots, p + 1$ .

In this paper we are interested in a subclass of GLMs (2.2) with the following properties:

- The GLM (2.2) has order  $p$  and stage order  $q = p$ .
- The number of external stages  $r$  and the number of internal stages  $s$  are equal to  $r = s = p + 1$ .
- The GLM (2.2) is nonconfluent, i.e., the abscissa vector  $\mathbf{c} = [c_1, c_2, \dots, c_s]^T$  satisfies  $c_i \neq c_j$  for  $i \neq j$ .
- The GLM (2.2) satisfies the preconsistency conditions (2.8).
- The coefficient matrix  $\mathbf{A}$  is lower triangular with diagonal elements each equal to  $\lambda \geq 0$ .
- The vectors  $\mathbf{y}^{[n]}$  and  $\mathbf{y}^{[n+1]}$  are approximations of order  $p$  to the Nordsieck vectors  $\mathbf{z}(t_n, h)$  and  $\mathbf{z}(t_{n+1}, h)$ , respectively. This implies that the vectors  $\mathbf{q}_k$  are equal to  $\mathbf{q}_0 = \mathbf{e}_1, \mathbf{q}_1 = \mathbf{e}_2, \dots, \mathbf{q}_p = \mathbf{e}_{p+1}$ , where  $\mathbf{e}_1, \mathbf{e}_2, \dots, \mathbf{e}_{p+1}$  is the canonical basis of the space  $\mathbb{R}^{p+1}$ .
- The method (2.2) satisfies IRKS properties (3.5), (3.6), and (3.7), with the doubly companion matrix  $\mathbf{X}$  of the form (3.8) which has a one point spectrum  $\sigma(\mathbf{X}) = \{\lambda\}$ , where  $\lambda$  is the diagonal element of the coefficient matrix  $\mathbf{A}$ .

The GLMs which satisfy the above conditions have been introduced in [17,46], and further investigated in [15,33,47]. In particular, they have RK stability, i.e., their stability function  $p(w, z)$  satisfies the condition (3.4). Moreover, as demonstrated in [17,46] (see also [33]) the stability function  $R(z)$  appearing in (3.4) has the form

$$R(z) = \frac{P(z)}{(1 - \lambda z)^{p+1}}, \tag{3.9}$$

where

$$\begin{aligned} P(z) &= \exp(z)(1 - \lambda z)^{p+1} - Ez^{p+1} + O(z^{p+2}) \\ &= \sum_{n=0}^p M_{n,p+1}(\lambda)z^n + \epsilon z^{p+1}, \end{aligned} \tag{3.10}$$

and

$$\epsilon = M_{p+1,p+1}(\lambda) - E. \tag{3.11}$$

Here,  $E$  is the error constant of the method and the polynomials  $M_{n,m}(\lambda)$  are defined by

$$M_{n,m}(\lambda) = \sum_{i=0}^n \binom{m}{i} \frac{(-\lambda)^i}{(n-i)!}. \tag{3.12}$$

We will also define polynomials  $N_i(\lambda)$  by the formula

$$N_i(\lambda) = \sum_{k=0}^{i-1} \binom{i-1}{k} \frac{(-\lambda)^k}{(i-k)!}. \tag{3.13}$$

As in [33] let us partition the coefficient matrices  $\mathbf{A}$ ,  $\mathbf{U}$ ,  $\mathbf{B}$ , and  $\mathbf{V}$  as follows

$$\left[ \begin{array}{c|c} \mathbf{A} & \mathbf{U} \\ \mathbf{B} & \mathbf{V} \end{array} \right] = \left[ \begin{array}{c|c} \mathbf{A} & \mathbf{e} \ U \\ \mathbf{b}^T & 1 \ \mathbf{v}^T \\ \mathbf{B} & \mathbf{0} \ V \end{array} \right],$$

where  $\mathbf{e} = [1, 1, \dots, 1]^T \in \mathbb{R}^s$ ,  $\mathbf{b} \in \mathbb{R}^s$ ,  $\mathbf{v} \in \mathbb{R}^{s-1}$ ,  $\mathbf{U} \in \mathbb{R}^{s \times (s-1)}$ ,  $\mathbf{B} \in \mathbb{R}^{(s-1) \times s}$ ,  $\mathbf{V} \in \mathbb{R}^{(s-1) \times (s-1)}$ . Then the error constant  $E$  of GLM (2.2) is given by

$$E = \frac{1}{(p+1)!} - \frac{\mathbf{b}^T \mathbf{c}^p}{p!} + \mathbf{v}^T \theta, \tag{3.14}$$

where

$$\theta = (\mathbf{I} - \mathbf{V})^{-1} \left( \mathbf{t}_p - \mathbf{B} \frac{\mathbf{c}^p}{p!} \right), \quad \mathbf{t}_p = \left[ \frac{1}{p!} \ \frac{1}{(p-1)!} \ \dots \ \frac{1}{1!} \right]^T,$$

compare [16,33].

It is quite remarkable that the explicit or implicit GLMs of any order with the properties listed above can be constructed using only linear operations. Such an algorithm for construction of these methods, which was discovered by Butcher and Wright [17,46], is described in the next section.

### 4 Algorithm for Construction of GLMs with IRKS

In this section we describe the practical algorithm, discovered by Butcher and Wright [17,46], for the construction of GLMs with IRKS which have properties discussed in Sect. 3. Since the construction of extrapolated IMEX schemes starts with an implicit GLM, we describe this algorithm adapted to the case of diagonally implicit GLMs. As in [17,33,46] we introduce the following notation. For a square matrix  $\Omega$  we denote by  $\Delta(\Omega)$  the lower triangular part of the matrix  $\Omega$ , which includes also the diagonal. We also use the notation  $\mathcal{L}(\Omega)$  and  $\mathcal{U}(\Omega)$  for unit lower triangular and upper triangular matrix, respectively, such that  $\Omega = \mathcal{L}(\Omega)\mathcal{U}(\Omega)$ , assuming that this LU decomposition exists.

The description of the algorithm, which is presented below, for construction of GLMs with IRKS and the properties specified in Sect. 3, follows closely the presentation in the monograph [33]. This algorithm consists of the following steps.

1. Choose the order  $p$  and the vector  $\mathbf{c} = [c_1, c_2, \dots, c_s]^T \in \mathbb{R}^s$ ,  $s = p + 1$ , with distinct abscissas  $c_i$ . It is usually assumed that  $0 \leq c_i \leq 1$ ,  $i = 1, 2, \dots, s$ . The typical choice are abscissas uniformly distributed on the interval  $[0, 1]$ , i.e.,  $c_i = (i - 1)/(s - 1)$ ,  $i = 1, 2, \dots, s$ .
2. Choose the diagonal element  $\lambda$  of the coefficient matrix  $\mathbf{A}$ . This parameter is usually chosen in such a way that the resulting GLM with stability function  $R(z)$  given by (3.9), where the numerator  $P(z)$  is given by (3.10), is  $A$ -stable.
3. Choose the  $z^{p+1}$  coefficient  $\epsilon$  of the numerator  $P(z)$  given by (3.10) of the stability function  $R(z)$  (3.9). Choosing  $\epsilon = 0$  leads to methods which are  $L$ -stable.
4. Choose the parameters  $\beta_1, \beta_2, \dots, \beta_p$  appearing in the doubly companion matrix  $\mathbf{X}$  (3.8). In this paper we consider two strategies for choosing these parameters. The first strategy is based on choosing these parameters by maximizing the area of stability of the explicit GLM or of the IMEX scheme assuming that the implicit part of the method is  $A(\alpha)$ -stable for some  $0 < \alpha \leq \pi/2$ , preferably for  $\alpha = \pi/2$ . The second strategy

consists of assuming that  $\beta_1 = \beta_2 = \dots = \beta_p = E$ , where  $E$  is the error constant of the method. The rationale for his strategy was given in [15], see also [17,33,46].

5. Compute the matrix  $\Psi = \beta(\mathbf{K}) \exp(\lambda \mathbf{K}^-)$ , where

$$\mathbf{K} = \begin{bmatrix} 0 & 1 & 0 & \dots & 0 \\ 0 & 0 & 1 & \dots & 0 \\ \vdots & \vdots & \vdots & \ddots & \vdots \\ 0 & 0 & 0 & \dots & 1 \\ 0 & 0 & 0 & \dots & 0 \end{bmatrix}, \quad \mathbf{K}^- = \begin{bmatrix} 0 & p & 0 & \dots & 0 & 0 & 0 \\ 0 & 0 & p-1 & \dots & 0 & 0 & 0 \\ 0 & 0 & 0 & \ddots & 0 & 0 & 0 \\ \vdots & \vdots & \vdots & \ddots & \ddots & \vdots & \vdots \\ 0 & 0 & 0 & \dots & 0 & 2 & 0 \\ 0 & 0 & 0 & \dots & 0 & 0 & 1 \\ 0 & 0 & 0 & \dots & 0 & 0 & 0 \end{bmatrix},$$

$\mathbf{K}, \mathbf{K}^- \in \mathbb{R}^{(p+1) \times (p+1)}$ , and

$$\beta(\mathbf{K}) := \beta_1 \mathbf{K} + \beta_2 \mathbf{K}^2 + \dots + \beta_{p+1} \mathbf{K}^{p+1} \in \mathbb{R}^{(p+1) \times (p+1)}.$$

6. Compute the matrix  $\mathbf{X} = \Psi(\mathbf{J} + \lambda \mathbf{I})\Psi^{-1}$ , where  $\mathbf{J} = \mathbf{K}^T$ . Then, clearly, this matrix has a one point spectrum  $\sigma(\mathbf{X}) = \{\lambda\}$ . Moreover, as demonstrated in [17,46] (see also [33]), this matrix has a doubly companion form (3.8).
7. Compute the matrix  $\mathbf{F} = \exp(-\lambda \mathbf{K}^-) \exp(\mathbf{K}) \exp(\lambda \mathbf{K}^-)$ .
8. Compute the matrix  $\Omega = \mathbf{C} (\beta(\mathbf{K}) \mathbf{e}_{p+1} \mathbf{e}_1^T + \mathbf{K} \Psi)$ , where

$$\mathbf{C} = \begin{bmatrix} \mathbf{e} & \mathbf{c} & \frac{\mathbf{c}^2}{2!} & \dots & \frac{\mathbf{c}^p}{p!} \end{bmatrix} \in \mathbb{R}^{(p+1) \times (p+1)}.$$

9. Compute the matrix  $\Gamma = \mathbf{I}_r \mathbf{I}_c \mathbf{F} \mathbf{I}_r \mathbf{I}_c + \delta \mathbf{e}_1^T$ , where

$$\mathbf{I}_r = \begin{bmatrix} \mathbf{0} \\ \mathbf{I} \end{bmatrix} \in \mathbb{R}^{(p+1) \times p}, \quad \mathbf{I}_c = [\mathbf{0} | \mathbf{I}] \in \mathbb{R}^{p \times (p+1)},$$

$\mathbf{0}$  is a row or column vector of dimension  $p$ , and  $\mathbf{I} \in \mathbb{R}^{p \times p}$  is the identity matrix. Moreover, the vector  $\delta$  is given by

$$\delta = [\epsilon + \lambda M_{p,p}(\lambda) N_p(\lambda) \dots N_1(\lambda)]^T \in \mathbb{R}^{p+1},$$

where the polynomial  $M_{p,p}(\lambda)$  is defined by (3.12), and the polynomials  $N_k(\lambda)$ ,  $k = 1, 2, \dots, p$ , are defined by (3.13).

10. Choose a unit lower triangular matrix  $L \in \mathbb{R}^{p \times p}$  and compute the LU decomposition of the matrix  $\Omega \mathbf{L} = \mathcal{L}(\Omega \mathbf{L}) \mathcal{U}(\Omega \mathbf{L})$ , where

$$\mathbf{L} = \begin{bmatrix} 1 & | & \mathbf{0} \\ \mathbf{0} & | & L \end{bmatrix} \in \mathbb{R}^{(p+1) \times (p+1)}.$$

11. Compute the matrix  $\tilde{\mathbf{B}}$  from  $\tilde{\mathbf{B}} = \mathbf{L} \Delta (\mathbf{L}^{-1} \Gamma \mathcal{L} \mathcal{U}(\Omega \mathbf{L})^{-1}) \mathcal{L}(\Omega \mathbf{L})^{-1}$ .
12. Compute the coefficient matrices  $\mathbf{B}, \mathbf{A}, \mathbf{U}$ , and  $\mathbf{V}$  of GLM (2.2) from the formulas  $\mathbf{B} = \Psi \tilde{\mathbf{B}}, \mathbf{A} = \mathbf{B}^{-1} \mathbf{X} \mathbf{B}, \mathbf{U} = \mathbf{C} - \mathbf{A} \mathbf{C} \mathbf{K}, \mathbf{V} = \exp(\mathbf{K}) - \mathbf{B} \mathbf{C} \mathbf{K}$ .

We would like to reiterate again that the GLM with abscissa vector  $\mathbf{c}$  and coefficients matrices  $\mathbf{A}, \mathbf{U}, \mathbf{B}$ , and  $\mathbf{V}$ , computed by the above algorithm has IRKS and the properties given in Sect. 3.

This algorithm will fail if the matrix  $\Omega \mathbf{L}$  is singular or it does not admit LU decomposition, or if the matrix  $\tilde{\mathbf{B}}$ , and as a result the matrix  $\mathbf{B}$ , is singular. However, it was demonstrated in [15,17,33,46,47] that the overall algorithm can be carried out successfully for many choices

of the abscissa vector  $\mathbf{c}$ , the parameter  $\lambda$ , the coefficient  $\epsilon$ , the parameters  $\beta_1, \beta_2, \dots, \beta_s$ , and the unit lower triangular matrix  $L$ . The examples of implicit GLMs with IRKS obtained by this algorithm are given in Sect. 8.

### 5 Extrapolated IMEX GLMs with IRKS

In this section we follow the approach, first proposed by Cardone et al. in the case of IMEX DIMSIMS [19,20] and IMEX RK methods [21], to derive new extrapolation-based GLMs with IRKS. Assume that the GLM (2.2) is derived using the algorithm presented in Sect. 4, i.e., it has IRKS and additional properties listed in Sect. 3. As in [19–21] consider the extrapolation formula for  $f_j^{[n+1]}$  depending on stage values  $Y_k^{[n]}, k = 1, 2, \dots, s$ , and  $Y_k^{[n+1]}, k = 1, 2, \dots, j - 1$ , at two consecutive steps

$$f_j^{[n+1]} = \sum_{k=1}^s \alpha_{jk} f(Y_k^{[n]}) + \sum_{k=1}^{j-1} \beta_{jk} f(Y_k^{[n+1]}), \quad j = 1, 2, \dots, s. \tag{5.1}$$

As in [19,20], substituting (5.1) into (1.2), then changing the order of summation in the resulting double sums, and interchanging the indices  $j$  and  $k$  leads to the class of IMEX GLMs with IRKS of the form

$$\left\{ \begin{aligned} Y_i^{[n+1]} &= h \sum_{j=1}^s \bar{a}_{ij} f(Y_j^{[n]}) + h \sum_{j=1}^{i-1} a_{ij}^* f(Y_j^{[n+1]}) \\ &\quad + h \sum_{j=1}^i a_{ij} g(Y_j^{[n+1]}) + \sum_{j=1}^r u_{ij} y_j^{[n]}, \quad i = 1, 2, \dots, s, \\ y_i^{[n+1]} &= h \sum_{j=1}^s \bar{b}_{ij} f(Y_j^{[n]}) + h \sum_{j=1}^{s-1} b_{ij}^* f(Y_j^{[n+1]}) \\ &\quad + h \sum_{j=1}^s b_{ij} g(Y_j^{[n+1]}) + \sum_{j=1}^r v_{ij} y_j^{[n]}, \quad i = 1, 2, \dots, r, \end{aligned} \right. \tag{5.2}$$

$n = 0, 1, \dots, N - 1$ . Here, the coefficients  $\bar{a}_{ij}, a_{ij}^*, \bar{b}_{ij}$ , and  $b_{ij}^*$  are defined by

$$\bar{a}_{ij} = \sum_{k=1}^i a_{ik} \alpha_{kj}, \quad a_{ij}^* = \sum_{k=j+1}^i a_{ik} \beta_{kj}, \quad \bar{b}_{ij} = \sum_{k=1}^s b_{ik} \alpha_{kj}, \quad b_{ij}^* = \sum_{k=j+1}^s b_{ik} \beta_{kj}.$$

Put  $\bar{\mathbf{A}} = [\bar{a}_{ij}] \in \mathbb{R}^{s \times s}$ ,  $\mathbf{A}^* = [a_{ij}^*] \in \mathbb{R}^{s \times s}$ ,  $\bar{\mathbf{B}} = [\bar{b}_{ij}] \in \mathbb{R}^{r \times s}$ ,  $\mathbf{B}^* = [b_{ij}^*] \in \mathbb{R}^{r \times s}$ ,  $\alpha = [\alpha_{ij}] \in \mathbb{R}^{s \times s}$ ,  $\beta = [\beta_{ij}] \in \mathbb{R}^{s \times s}$ . Then

$$\bar{\mathbf{A}} = \mathbf{A} \alpha, \quad \mathbf{A}^* = \mathbf{A} \beta, \quad \bar{\mathbf{B}} = \mathbf{B} \alpha, \quad \mathbf{B}^* = \mathbf{B} \beta. \tag{5.3}$$



Observe that the matrix  $\mathbf{A}^*$  is strictly lower triangular and that the last column of the matrix  $\mathbf{B}^*$  is equal to a zero vector. Introducing the notation

$$Y^{[n]} = \begin{bmatrix} Y_1^{[n]} \\ \vdots \\ Y_s^{[n]} \end{bmatrix}, \quad y^{[n]} = \begin{bmatrix} y_1^{[n]} \\ \vdots \\ y_r^{[n]} \end{bmatrix},$$

$$f(Y^{[n]}) = \begin{bmatrix} f(Y_1^{[n]}) \\ \vdots \\ f(Y_s^{[n]}) \end{bmatrix}, \quad g(y^{[n]}) = \begin{bmatrix} g(y_1^{[n]}) \\ \vdots \\ g(y_r^{[n]}) \end{bmatrix},$$

the IMEX method (5.2) can be written in a more compact vector form

$$\begin{cases} Y^{[n+1]} = h(\bar{\mathbf{A}} \otimes \mathbf{I})f(Y^{[n]}) + h(\mathbf{A}^* \otimes \mathbf{I})f(Y^{[n+1]}) \\ \quad + h(\mathbf{A} \otimes \mathbf{I})g(Y^{[n+1]}) + (\mathbf{U} \otimes \mathbf{I})y^{[n]}, \\ y^{[n+1]} = h(\bar{\mathbf{B}} \otimes \mathbf{I})f(Y^{[n]}) + h(\mathbf{B}^* \otimes \mathbf{I})f(Y^{[n+1]}) \\ \quad + h(\mathbf{B} \otimes \mathbf{I})g(Y^{[n+1]}) + (\mathbf{V} \otimes \mathbf{I})y^{[n]}, \end{cases} \tag{5.4}$$

$n = 0, 1, \dots, N - 1$ , where  $\mathbf{I}$  is the identity matrix of dimension  $m$ .

Assuming that  $g(y) = 0$  we obtain a two-step method of the form

$$\begin{cases} Y^{[n+1]} = h(\bar{\mathbf{A}} \otimes \mathbf{I})f(Y^{[n]}) + h(\mathbf{A}^* \otimes \mathbf{I})f(Y^{[n+1]}) + (\mathbf{U} \otimes \mathbf{I})y^{[n]}, \\ y^{[n+1]} = h(\bar{\mathbf{B}} \otimes \mathbf{I})f(Y^{[n]}) + h(\mathbf{B}^* \otimes \mathbf{I})f(Y^{[n+1]}) + (\mathbf{V} \otimes \mathbf{I})y^{[n]}, \end{cases} \tag{5.5}$$

$n = 0, 1, \dots, N - 1$ . This two-step method can be represented as a single GLM extended over two steps from  $t_{n-1}$  to  $t_n$  and from  $t_n$  to  $t_{n+1}$  with the abscissa vector  $\tilde{\mathbf{c}} = [(\mathbf{c} - \mathbf{e})^T, \mathbf{c}^T]^T$  and

$$\begin{bmatrix} Y^{[n]} \\ Y^{[n+1]} \\ Y^{[n+1]} \\ y^{[n+1]} \end{bmatrix} = \left[ \begin{array}{cc|cc} \mathbf{0} & \mathbf{0} & \mathbf{I} & \mathbf{0} \\ \bar{\mathbf{A}} \otimes \mathbf{I} & \mathbf{A}^* \otimes \mathbf{I} & \mathbf{0} & \mathbf{U} \otimes \mathbf{I} \\ \mathbf{A} \otimes \mathbf{I} & \mathbf{A}^* \otimes \mathbf{I} & \mathbf{0} & \mathbf{U} \otimes \mathbf{I} \\ \bar{\mathbf{B}} \otimes \mathbf{I} & \mathbf{B}^* \otimes \mathbf{I} & \mathbf{0} & \mathbf{V} \otimes \mathbf{I} \end{array} \right] \begin{bmatrix} hf(Y^{[n]}) \\ hf(Y^{[n+1]}) \\ Y^{[n]} \\ y^{[n]} \end{bmatrix}. \tag{5.6}$$

Here,  $\mathbf{0}$  stands for the zero matrix of dimension  $ms \times ms$  and  $\mathbf{I}$  in the first row is the identity matrix of dimension  $ms$ .

Assuming that  $f(y) = 0$  the IMEX scheme (5.4) reduces to the underlying GLM (2.2).

A different approach to the construction of IMEX GLMs is discussed in [4, 22, 34, 49, 50]. IMEX Runge–Kutta methods are discussed in [1, 2, 18, 29, 30, 35, 38, 39, 42], and IMEX linear multistep methods in [3, 23, 25, 29]. IMEX two-step Runge–Kutta methods are discussed in the paper [51].

## 6 Convergence and Error Analysis of IMEX GLMs

In this section we present error analysis of the interpolation formula defined by (5.1), investigate order of convergence of IMEX scheme (5.4), and discuss Prothero–Robinson convergence of (5.4).

### 6.1 Error Analysis for the Interpolant

As in [19, 20] we define the local discretization error  $\eta(t_n + c_j h)$  of the extrapolation formula (5.1) as the residuum obtained by replacing in (5.1)  $f_j^{[n+1]}$  by  $f(y(t_n + c_j h))$ ,  $Y_k^{[n]}$  by

$y(t_{n-1} + c_k h)$ , and  $Y_k^{[n+1]}$  by  $y(t_n + c_k h)$ . This leads to

$$f(y(t_n + c_j h)) = \sum_{k=1}^s \alpha_{ij} f(y(t_{n-1} + c_k h)) + \sum_{k=1}^{j-1} \beta_{jk} f(y(t_n + c_k h)) + \eta(t_n + c_j h), \tag{6.1}$$

$j = 1, 2, \dots, s$ . Putting  $\varphi(t) = f(y(t))$  (6.1) can be written in the form

$$\eta(t_n + c_j h) = \varphi(t_n + c_j h) - \sum_{k=1}^s \alpha_{jk} \varphi(t_{n-1} + c_k h) - \sum_{k=1}^{j-1} \beta_{jk} \varphi(t_n + c_k h),$$

$j = 1, 2, \dots, s$ . Expanding  $\varphi(t_n + c_j h)$ ,  $\varphi(t_n + (c_k - 1)h)$ , and  $\varphi(t_n + c_k h)$  into Taylor series around  $t_n$  leads to

$$\eta(t_n + c_j h) = \sum_{l=0}^p \left( \frac{c_j^l}{l!} - \sum_{k=1}^s \alpha_{jk} \frac{(c_k - 1)^l}{l!} - \sum_{k=1}^{j-1} \beta_{jk} \frac{c_k^l}{l!} \right) h^l \varphi^{(l)}(t_n) + O(h^{p+1}).$$

We assume that the extrapolation procedure given by (5.1) has order  $p$ , i.e.,  $\eta(t_n + c_j h) = O(h^p)$ . This leads to the system of equations for the coefficients  $\alpha_{jk}$  and  $\beta_{jk}$

$$\sum_{k=1}^s \alpha_{jk} (c_k - 1)^l = c_j^l - \sum_{k=1}^{j-1} \beta_{jk} c_k^l,$$

$l = 0, 1, \dots, p - 1, j = 1, 2, \dots, s$ , or in vector form

$$\alpha(\mathbf{c} - \mathbf{e})^l = (\mathbf{I} - \beta)\mathbf{c}^l, \quad l = 0, 1, \dots, p - 1. \tag{6.2}$$

For methods with  $s = p + 1$  this is a system of  $sp = s(s - 1)$  equations, and we will solve it with respect to  $\alpha_{jk}, j = 1, 2, \dots, s, k = 1, 2, \dots, s - 1$ , i.e., with respect to the first  $s - 1$  columns of the coefficient matrix  $\alpha$ . Putting

$$\mathbf{Q} = [\mathbf{e} \ \mathbf{c} - \mathbf{e} \ (\mathbf{c} - \mathbf{e})^2 \ \dots \ (\mathbf{c} - \mathbf{e})^{p-1}] \in \mathbb{R}^{s \times (s-1)},$$

$$\tilde{\mathbf{C}} = [\mathbf{e} \ \mathbf{c} \ \mathbf{c}^2 \ \dots \ \mathbf{c}^{p-1}] \in \mathbb{R}^{s \times (s-1)},$$

the system (6.2) can be rewritten as

$$\alpha \mathbf{Q} = (\mathbf{I} - \beta)\tilde{\mathbf{C}}. \tag{6.3}$$

Partitioning the matrices  $\alpha$  and  $\mathbf{Q}$  in the form

$$\alpha = [\tilde{\alpha} | \alpha^*], \quad \mathbf{Q} = \begin{bmatrix} \tilde{\mathbf{Q}} \\ \mathbf{Q}^* \end{bmatrix},$$

where  $\tilde{\alpha} \in \mathbb{R}^{s \times (s-1)}, \alpha^* \in \mathbb{R}^{s \times 1}, \tilde{\mathbf{Q}} \in \mathbb{R}^{(s-1) \times (s-1)}$ , and  $\mathbf{Q}^* \in \mathbb{R}^{1 \times (s-1)}$ , the system (6.3) takes the form  $\tilde{\alpha} \tilde{\mathbf{Q}} + \alpha^* \mathbf{Q}^* = (\mathbf{I} - \beta)\tilde{\mathbf{C}}$ . This leads to

$$\tilde{\alpha} = ((\mathbf{I} - \beta)\tilde{\mathbf{C}} - \alpha^* \mathbf{Q}^*) \tilde{\mathbf{Q}}^{-1}. \tag{6.4}$$

### 6.2 Convergence and Order Analysis of IMEX Scheme

To analyze the order and stage order of IMEX GLMs (5.2) we will impose some conditions on the local discretization errors of the internal and external stages of the underlying GLM (2.2) and on the accuracy of the extrapolation procedure (5.1). These local discretization errors  $hd(t_n + c_i h)$  and  $h\widehat{d}(t_{n+1})$  of the internal and external stages  $Y_i^{[n+1]}$  and  $y_i^{[n+1]}$  of the GLM (2.2) are defined as the residua obtained by substitution into (2.2) of  $y(t_n + c_i h)$  instead of  $Y_i^{[n+1]}$ ,  $z_j(t_n, h)$  instead of  $y_j^{[n]}$ , and  $z_j(t_{n+1}, h)$  instead of  $y_j^{[n+1]}$ , where  $z_j(t, h)$  are components of the Nordsieck vector defined by (2.5). This leads to

$$y(t_n + c_i h) = h \sum_{j=1}^i a_{ij} y'(t_n + c_j h) + \sum_{j=1}^r u_{ij} z_j(t_n, h) + hd(t_n + c_i h), \tag{6.5}$$

$i = 1, 2, \dots, s$ , and

$$z_i(t_{n+1}, h) = h \sum_{j=1}^s b_{ij} y'(t_n + c_j h) + \sum_{j=1}^r v_{ij} z_j(t_n, h) + h\widehat{d}(t_{n+1}), \tag{6.6}$$

$i = 1, 2, \dots, r$ . In this paper we will examine only methods of order  $p$  and stage order  $q = p$ , i.e., methods which satisfy the conditions  $h\widehat{d}(t_{n+1}) = O(h^{p+1})$ , and  $hd(t_n + c_i h) = O(h^{q+1})$ ,  $i = 1, 2, \dots, s$ , where  $q = p$ . The order and stage order conditions for such GLMs can be obtained by expanding  $y(t_n + c_i h)$ ,  $y'(t_n + c_j h)$ ,  $z_i(t_n, h)$ , and  $z_i(t_{n+1}, h)$  in (6.5) and (6.6) into Taylor series around the point  $t_n$  and comparing to zero the coefficients of the successive powers of  $h$  up to the required order. These order and stage order conditions were derived in [11] and [14] (compare also [33]), using the theory of functions of a complex variable  $z$ , and they are listed as conditions (2.6) and (2.7) in Sect. 2.

Similarly as in the case of GLMs (2.2) we define the local discretization errors  $h\xi(t_n + c_i h)$  and  $h\widehat{\xi}(t_{n+1})$  of internal and external approximations  $Y_i^{[n+1]}$  and  $y_i^{[n+1]}$  of IMEX GLMs (5.2) or (5.4) by the relations

$$y(t_n + c_i h) = h \sum_{j=1}^s \bar{a}_{ij} f(y(t_n + c_j h)) + h \sum_{j=1}^{i-1} a_{ij}^* f(y(t_n + c_j h)) + h \sum_{j=1}^i a_{ij} g(y(t_n + c_j h)) + \sum_{j=1}^r u_{ij} z_j(t_n, h) + h\xi(t_n + c_i h), \tag{6.7}$$

$j = 1, 2, \dots, s$ , and

$$z_i(t_{n+1}, h) = h \sum_{j=1}^s \bar{b}_{ij} f(y(t_n + c_j h)) + h \sum_{j=1}^{s-1} b_{ij}^* f(y(t_n + c_j h)) + h \sum_{j=1}^s b_{ij} g(y(t_n + c_j h)) + \sum_{j=1}^r v_{ij} z_j(t_n, h) + h\widehat{\xi}(t_{n+1}), \tag{6.8}$$

$i = 1, 2, \dots, r$ . Then the IMEX GLM (5.2) has order  $p$  and stage order  $q = p$  if and only if  $h\widehat{\xi}(t_{n+1}) = O(h^{p+1})$ , and  $h\xi(t_n + c_i h) = O(h^{p+1})$ ,  $i = 1, 2, \dots, s$ . We have the following theorem.

**Theorem 1** Assume that GLM (2.2) has order  $p$  and stage order  $q = p$ , and that the extrapolation procedure (5.1) has order  $p$ , i.e.,  $\eta(t_n + c_j h) = O(h^p)$ ,  $j = 1, 2, \dots, s$ . Then the IMEX GLM (5.2) has order  $p$  and stage order  $q = p$ .

*Proof* This theorem follows from [50] or [20], but for the sake of completeness we present below a somewhat simpler, new proof of this result.

Using the definitions of  $\bar{a}_{ij}$ ,  $a_{ij}^*$ ,  $\bar{b}_{ij}$ ,  $b_{ij}^*$ , and reversing the process which led to the derivation of IMEX GLMs (5.2) we obtain

$$y(t_n + c_i h) = h \sum_{j=1}^i a_{ij} \left( \sum_{k=1}^s \alpha_{jk} f(y(t_{n-1} + c_k h)) + \sum_{k=1}^{j-1} \beta_{kj} f(y(t_n + c_k h)) \right) + h \sum_{j=1}^s a_{ij} g(y(t_n + c_j h)) + \sum_{j=1}^r u_{ij} z_j(t_n, h) + h \xi(t_n + c_i h),$$

$i = 1, 2, \dots, s$ , and

$$z_i(t_{n+1}, h) = h \sum_{j=1}^s b_{ij} \left( \sum_{k=1}^s \alpha_{jk} f(y(t_{n-1} + c_k h)) + \sum_{k=1}^{j-1} \beta_{kj} f(y(t_n + c_k h)) \right) + h \sum_{j=1}^s b_{ij} g(y(t_n + c_j h)) + \sum_{j=1}^r v_{ij} z_j(t_n, h) + h \widehat{\xi}(t_{n+1}),$$

$i = 1, 2, \dots, r$ . Taking into account (6.1) and the relations

$$y'(t_n + c_j h) = f(y(t_n + c_j h)) + g(y(t_n + c_j h)), \quad j = 1, 2, \dots, s,$$

leads to

$$y(t_n + c_i h) = h \sum_{j=1}^i a_{ij} y'(t_n + c_j h) + \sum_{j=1}^r u_{ij} z_j(t_n, h) - h \sum_{j=1}^i a_{ij} \eta(t_n + c_j h) + h \xi(t_n + c_i h),$$

$i = 1, 2, \dots, s$ , and

$$z_i(t_{n+1}, h) = h \sum_{j=1}^s b_{ij} y'(t_n + c_j h) + \sum_{j=1}^r v_{ij} z_j(t_n, h) - h \sum_{j=1}^s b_{ij} \eta(t_n + c_j h) + h \widehat{\xi}(t_{n+1}),$$

$i = 1, 2, \dots, r$ . Using the relations (6.5) and (6.6) which define local discretization errors of GLM (2.2) it follows that

$$h \xi(t_n + c_i h) = h d(t_n + c_i h) + h \sum_{j=1}^i a_{ij} \eta(t_n + c_j h),$$

$i = 1, 2, \dots, s$ , and

$$h \widehat{\xi}(t_{n+1}) = h \widehat{d}(t_{n+1}) + h \sum_{j=1}^s b_{ij} \eta(t_n + c_j h),$$

$i = 1, 2, \dots, r$ . Hence, the relations  $d(t_n + c_i h) = O(h^{p+1})$ ,  $h \widehat{d}(t_{n+1}) = O(h^{p+1})$ , and  $\eta(t_n + c_j h) = O(h^p)$ , imply that  $h \xi(t_n + c_i h) = O(h^{p+1})$ , and  $h \widehat{\xi}(t_{n+1}) = O(h^{p+1})$ . This shows that the IMEX GLM (5.2) has order  $p$  and stage order  $q = p$ .  $\square$

### 6.3 Prothero–Robinson Convergence of IMEX GLMs

We will demonstrate in this section that contrary to the methods of low stage order, the IMEX schemes (5.2) considered in this paper, do not suffer from order reduction phenomenon when applied to stiff systems of differential equations. Following [10, 50, 51] we consider the Prothero–Robinson (PR) [41] test problem of the form

$$\begin{cases} y'(t) = \mu (y(t) - \phi(t)) + \phi'(t), & t \geq 0, \\ y(0) = \phi(0), \end{cases} \tag{6.9}$$

where  $\mu \in \mathbb{C}$  has a large and negative real part and  $\phi(t)$  is a slowly varying function. Here,  $\phi'(t)$  corresponds to the non-stiff part and  $\mu(y(t) - \phi(t))$  to the stiff part of (6.9). The solution to (6.9) is  $y(t) = \phi(t)$ . The IMEX scheme (5.2) is said to be PR-convergent if the application of (5.2) to the Eq. (6.9) leads to the numerical solution  $y^{[n]}$  whose global error defined by

$$e_h(t_n) = \|y^{[n]} - \mathbf{z}(t_n, h)\|,$$

where  $\mathbf{z}(t, h)$  is the Nordsieck vector defined by (2.5), satisfies  $e_h(t_n) = O(h^p)$  as  $h \rightarrow 0$  and  $h\mu \rightarrow -\infty$ . The PR-convergence of Runge–Kutta formulas was investigated by Butcher [10], of a class of IMEX DIMSIMs by Zhang et al. [50], and of a class of IMEX two-step Runge–Kutta methods by Zharovsky et al. [51]. We have the following theorem.

**Theorem 2** *Assume that the implicit GLM (2.2) given by the abscissa vector  $\mathbf{c}$  and coefficient matrices  $\mathbf{A}$ ,  $\mathbf{U}$ ,  $\mathbf{B}$ , and  $\mathbf{V}$ , has order  $p$  and stage order  $q = p$ , and that the extrapolation formula (5.1) has order  $p$ , i.e.,  $\eta(t_n + c_j h) = O(h^p)$ ,  $j = 1, 2, \dots, s$ , where  $\eta(t_n + c_j h)$  is defined by (6.1). Then the IMEX scheme (5.2) is PR-convergent with order  $p$  as  $h \rightarrow 0$ ,  $h\mu \rightarrow -\infty$ , and  $h\mu \in \mathcal{S}_I$ . Here,  $\mathcal{S}_I$  is the stability region of the implicit GLM (2.2).*

*Proof* It was already observed in Sect. 5 that the explicit two-step method (5.5) corresponding to  $g(y) = 0$  can be written as a single GLM extended over two steps (5.6), where the matrices  $\bar{\mathbf{A}}$ ,  $\mathbf{A}^*$ ,  $\bar{\mathbf{B}}$ , and  $\mathbf{B}^*$  are defined in Sect. 5. It follows from Theorem 1 that this method has order  $p$  and stage order  $q = p$ . Similarly, the implicit part of the IMEX scheme (5.2) corresponding to  $f(y) = 0$  and extended over two steps from  $t_{n-1}$  to  $t_n$  and  $t_n$  to  $t_{n+1}$  assumes the form

$$\begin{bmatrix} Y^{[n]} \\ Y^{[n+1]} \\ \bar{Y}^{[n+1]} \\ y^{[n+1]} \end{bmatrix} = \begin{bmatrix} \mathbf{0} & \mathbf{0} & \mathbf{I} & \mathbf{0} \\ \mathbf{0} & \mathbf{A} \otimes \mathbf{I} & \mathbf{0} & \mathbf{U} \otimes \mathbf{I} \\ \mathbf{0} & \mathbf{A} \otimes \mathbf{I} & \mathbf{0} & \mathbf{U} \otimes \mathbf{I} \\ \mathbf{0} & \mathbf{B} \otimes \mathbf{I} & \mathbf{0} & \mathbf{V} \otimes \mathbf{I} \end{bmatrix} \begin{bmatrix} g(Y^{[n]}) \\ g(Y^{[n+1]}) \\ \bar{Y}^{[n]} \\ y^{[n]} \end{bmatrix}. \tag{6.10}$$

This method has also order  $p$  and stage order  $q = p$ . The explicit method (5.6) and the implicit method (6.10) have the same abscissa vector  $\tilde{\mathbf{c}}$  given by  $\tilde{\mathbf{c}} = [(\mathbf{c} - \mathbf{e})^T, \mathbf{c}^T]^T$ . Moreover, the explicit method (5.6) and the implicit method (6.10) have the same matrices

$$\mathbf{U}^{exp} = \mathbf{U}^{imp} = \begin{bmatrix} \mathbf{I} & \mathbf{0} \\ \mathbf{0} & \mathbf{U} \end{bmatrix}, \quad \mathbf{V}^{exp} = \mathbf{V}^{imp} = \begin{bmatrix} \mathbf{0} & \mathbf{U} \\ \mathbf{0} & \mathbf{V} \end{bmatrix}.$$

It follows from these properties that the IMEX GLMs (5.2) form a partitioned GLM of the type considered by Zhang et al. in a recent paper [50]. Since as proved in [50], these partitioned methods are PR-convergent we can conclude that IMEX GLMs (5.2) are also PR-convergent with order  $p$ . This argument completes the proof of the theorem.  $\square$

### 7 Stability Analysis of IMEX GLMs

In this section we analyze stability properties of IMEX GLMs (5.2) with respect to the linear test equation

$$y'(t) = \lambda_0 y(t) + \lambda_1 y(t), \quad t \geq 0, \tag{7.1}$$

where  $\lambda_0$  and  $\lambda_1$  are complex parameters corresponding to the non-stiff  $f(y)$  and stiff  $g(y)$  parts of the system (1.1). Applying (5.2) to (7.1) and putting  $z_0 = h\lambda_0, z_1 = h\lambda_1$ , we obtain the vector recurrence relation of the form

$$\begin{bmatrix} Y^{[n+1]} \\ y^{[n+1]} \end{bmatrix} = \mathbf{M}(z_0, z_1) \begin{bmatrix} Y^{[n]} \\ y^{[n]} \end{bmatrix}, \tag{7.2}$$

with the stability matrix  $\mathbf{M}(z_0, z_1)$  defined by

$$\mathbf{M}(z_0, z_1) = \begin{bmatrix} m_{11}(z_0, z_1) & m_{12}(z_0, z_1) \\ m_{21}(z_0, z_1) & m_{22}(z_0, z_1) \end{bmatrix},$$

where

$$\begin{aligned} m_{11}(z_0, z_1) &= z_0 (\mathbf{I} - (z_0 \mathbf{A}^* + z_1 \mathbf{A}))^{-1} \bar{\mathbf{A}}, \\ m_{12}(z_0, z_1) &= (\mathbf{I} - (z_0 \mathbf{A}^* + z_1 \mathbf{A}))^{-1} \mathbf{U}, \\ m_{21}(z_0, z_1) &= z_0 (\bar{\mathbf{B}} + (z_0 \mathbf{B}^* + z_1 \mathbf{B}) (\mathbf{I} - (z_0 \mathbf{A}^* + z_1 \mathbf{A}))^{-1} \bar{\mathbf{A}}), \\ m_{22}(z_0, z_1) &= \mathbf{V} + (z_0 \mathbf{B}^* + z_1 \mathbf{B}) (\mathbf{I} - (z_0 \mathbf{A}^* + z_1 \mathbf{A}))^{-1} \mathbf{U}. \end{aligned}$$

Let  $\mathcal{S}_E \subset \mathbb{C}$  and  $\mathcal{S}_I \subset \mathbb{C}$  be the stability regions of the explicit GLM (5.6) and the implicit GLM (6.10), respectively. It was observed in [29] that large stability region of explicit method and desirable stability properties of the implicit method are not necessarily sufficient to guarantee good stability properties of the overall IMEX scheme (5.2). In practice it is necessary to investigate these stability properties when both explicit and implicit method operate in tandem as IMEX scheme (5.2). Following [50] we define the combined stability region of (5.2) by

$$\left\{ (z_0, z_1) \in \mathcal{S}_E \times \mathcal{S}_I : \rho(\mathbf{M}(z_0, z_1)) \leq 1 \right\} \subset \mathcal{S}_E \times \mathcal{S}_I \subset \mathbb{C} \times \mathbb{C}.$$

Here,  $\rho(\mathbf{M})$  stands for the spectral radius of  $\mathbf{M}$ . Then we define a desired stiff stability region, for example the region corresponding to implicit method which is  $A(\alpha)$ -stable for some  $\alpha \in (0, \pi/2]$ , i.e., the region given by

$$\mathcal{A}_\alpha = \left\{ z_1 \in \mathbb{C} : |\text{Im}(z_1)| \leq \tan(\alpha) |\text{Re}(z_1)| \right\},$$

and compute numerically the corresponding non-stiff region of the ‘explicit part’ of IMEX scheme (5.2), i.e., the region given by

$$\mathcal{S}_\alpha = \left\{ z_0 \in \mathbb{C} : \rho(\mathbf{M}(z_0, z_1)) \leq 1 \text{ for all } z_1 \in \mathcal{A}_\alpha \right\}.$$

It follows from the maximum principle for analytic functions [24] that this region has a simpler representation given by

$$\mathcal{S}_\alpha = \left\{ z_0 \in \mathbb{C} : \rho(\mathbf{M}(z_0, z_1)) \leq 1 \text{ for all } z_1 = -|y|/\tan(\alpha) + iy, y \in \mathbb{R} \right\}.$$

The boundary  $\partial \mathcal{S}_\alpha$  of  $\mathcal{S}_\alpha$  can be computed by the variant of boundary locus method which was described in [19–21]. This variant of boundary locus method is based on the relation

$\mathcal{S}_\alpha = \bigcap_{y \in \mathbb{R}} \mathcal{S}_{\alpha,y}$ , where

$$\mathcal{S}_{\alpha,y} = \left\{ z_0 \in \mathbb{C} : \rho(\mathbf{M}(z_0, z_1)) \leq 1 \text{ for fixed } z_1 = -|y|/\tan(\alpha) + iy \right\}.$$

Numerical techniques to compute numerically the region  $\mathcal{S}_\alpha$  were also discussed in [7, 29, 38]. Observe that the region  $\mathcal{S}_{\alpha,0}$  is independent of  $\alpha$  and that  $\mathcal{S}_{\alpha,0} = \mathcal{S}_E$ . We have  $\mathcal{S}_\alpha \subset \mathcal{S}_E$ , and we will try to construct IMEX GLMs (5.2) for which the intersection of the area of  $\mathcal{S}_\alpha$  with negative complex plane  $\mathbb{C}^-$  is as large as possible for fixed value of  $\alpha \in (0, \pi/2]$ , preferably for  $\alpha = \pi/2$ . The search for such IMEX schemes of order and stage order  $1 \leq p = q \leq 4$  is described in the next section.

### 8 Construction of Highly Stable IMEX GLMs

In this section we describe the construction of IMEX GLMs (5.2) with large areas of the intersection of  $\mathcal{S}_E$  and  $\mathcal{S}_\alpha$ , for some  $\alpha \in (0, \pi/2]$ , with negative complex plane  $\mathbb{C}^-$ . The construction starts with the derivation of implicit GLMs with IRKS and the properties discussed in Sect. 3, by the algorithm described in Sect. 4. Then we solve the minimization problems

$$- \text{area}(\mathcal{S}_E \cap \mathbb{C}^-) \longrightarrow \min, \tag{8.1}$$

or

$$- \text{area}(\mathcal{S}_\alpha \cap \mathbb{C}^-) \longrightarrow \min \tag{8.2}$$

for some  $\alpha \in (0, \pi/2]$ , with respect to the remaining free parameters of IMEX scheme (5.2). This is described in more details in Sects. 8.1–8.4.

#### 8.1 IMEX GLMs with $p = q = 1$ and $r = s = 2$

Choosing  $\mathbf{c} = [0, 1]^T$ ,  $\lambda = 1/2$ ,  $\epsilon = 0$ , and applying the algorithm described in Sect. 4 lead to the family of  $A$ - and  $L$ -stable GLMs with error constant  $E = -1/4$ , and coefficients depending on the free parameter  $\beta_1$

$$\left[ \begin{array}{c|c} \mathbf{A} & \mathbf{U} \\ \mathbf{B} & \mathbf{V} \end{array} \right] = \left[ \begin{array}{cc|cc} \frac{1}{2} & 0 & 1 & -\frac{1}{2} \\ \frac{1}{4\beta_1(\beta_1-1)} & \frac{1}{2} & 1 & \frac{1-2\beta_1+2\beta_1^2}{4\beta_1(\beta_1-1)} \\ \frac{1+2\beta_1^2+4\beta_1^3}{4\beta_1} & \frac{(\beta_1-1)(1+2\beta_1)}{2} & 1 & \frac{-1+2\beta_1-4\beta_1^2}{4\beta_1} \\ \beta_1 & 1-\beta_1 & 0 & 0 \end{array} \right].$$

We will search next for IMEX GLMs with maximal area of  $\mathcal{S}_E \cap \mathbb{C}^-$  and  $\mathcal{S}_\alpha \cap \mathbb{C}^-$  for  $\alpha = \pi/2$ . Computing the first column  $\tilde{\alpha}$  of the matrix  $\alpha$  appearing in the interpolation formula (5.1) from the formula (6.4) we obtain  $\alpha_{11} = 1 - \alpha_{12}$ ,  $\alpha_{21} = 1 - \alpha_{22} - \beta_{21}$ , where  $\alpha_{12}$ ,  $\alpha_{22}$ , and  $\beta_{21}$  are free parameters. Then solving the minimization problem (8.1) with respect to  $\alpha_{12}$ ,  $\alpha_{22}$ ,  $\beta_{21}$ , and  $\beta_1$ , we get

$$\begin{aligned} \alpha_{12} &= 0.2222226649982025, & \alpha_{22} &= -0.2956312425361826, \\ \beta_{21} &= 1.8879980487393651, & \beta_1 &= 0.7645871196918129, \end{aligned} \tag{8.3}$$

and for the corresponding IMEX GLM we have  $\text{area}(\mathcal{S}_E \cap \mathbb{C}^-) = 24.45$ ,  $\text{area}(\mathcal{S}_{\pi/2} \cap \mathbb{C}^-) = 16.49$ . We have plotted on Fig. 1 stability region  $\mathcal{S}_E$  (thick line), stability regions  $\mathcal{S}_{\pi/2,y}$  for  $y = -2.0, -1.6, \dots, 2.0$  (thin dotted lines), and stability region  $\mathcal{S}_{\pi/2}$  (shaded region), of the IMEX GLM corresponding to (8.3).

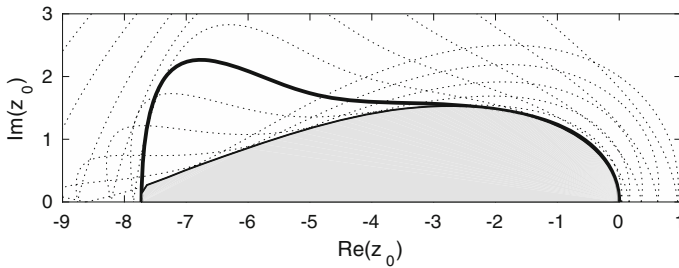


**Fig. 1** Stability region  $S_E$  (thick line),  $S_{\pi/2, y}$  for  $y = -2.0, -1.6, \dots, 2.0$  (thin dotted lines), and stability region  $S_{\pi/2}$  (shaded region), of the IMEX GLM corresponding to (8.3)

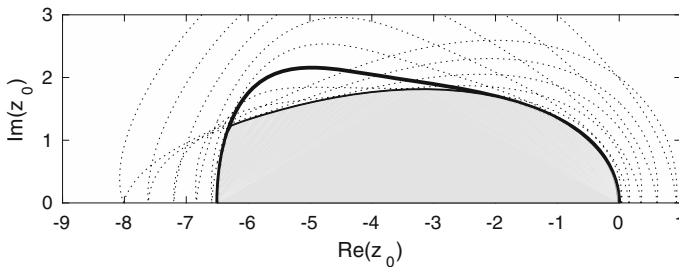


**Fig. 2** Stability region  $S_E$  (thick line),  $S_{\pi/2, y}$  for  $y = -2.0, -1.6, \dots, 2.0$  (thin dotted lines), and stability region  $S_{\pi/2}$  (shaded region), of the IMEX GLM corresponding to (8.4)

Solving instead of (8.1) the minimization problem (8.2) corresponding to  $\alpha = \pi/2$  we get

$$\begin{aligned} \alpha_{12} &= 0.2864217188168783, & \alpha_{22} &= -0.3291557174423694, \\ \beta_{21} &= 1.8454940193701925, & \beta_1 &= 0.7149171519838775, \end{aligned} \tag{8.4}$$

and for the corresponding IMEX GLM we have  $\text{area}(S_E \cap \mathbb{C}^-) = 21.75$ ,  $\text{area}(S_{\pi/2} \cap \mathbb{C}^-) = 19.19$ . We have plotted on Fig. 2 stability region  $S_E$  (thick line), stability regions  $S_{\pi/2, y}$  for  $y = -2.0, -1.6, \dots, 2.0$  (thin dotted lines), and stability region  $S_{\pi/2}$  (shaded region), of the IMEX GLM corresponding to (8.4).

We will assume next that  $\beta_1 = E = -1/4$ . Then the implicit GLM (2.2) takes the form

$$\left[ \begin{array}{c|c} \mathbf{A} & \mathbf{U} \\ \mathbf{B} & \mathbf{V} \end{array} \right] = \left[ \begin{array}{cc|cc} \frac{1}{2} & 0 & 1 & -\frac{1}{2} \\ -\frac{4}{5} & \frac{1}{2} & 1 & \frac{13}{10} \\ -\frac{17}{16} & \frac{5}{2} & 1 & \frac{7}{4} \\ -\frac{1}{4} & \frac{5}{4} & 0 & 0 \end{array} \right].$$

(Please note that there are some misprints in [33]). We will search again for IMEX GLMs with maximal area of  $S_E \cap \mathbb{C}^-$  and  $S_\alpha \cap \mathbb{C}^-$  for  $\alpha = \pi/2$ . Solving the minimization problem (8.1) with respect to  $\alpha_{12}$ ,  $\alpha_{22}$ , and  $\beta_{21}$ , we get

$$\begin{aligned} \alpha_{12} &= -0.1728737643890062, & \alpha_{22} &= 0.5728653112511124, \\ \beta_{21} &= 0.2634077885901063, \end{aligned} \tag{8.5}$$

and for the corresponding IMEX GLM we have that  $\text{area}(S_E \cap \mathbb{C}^-) = 4.50$ ,  $\text{area}(S_{\pi/2} \cap \mathbb{C}^-) = 2.58$ . We have plotted on Fig. 3 stability region  $S_E$  (thick line), stability regions  $S_{\pi/2, y}$



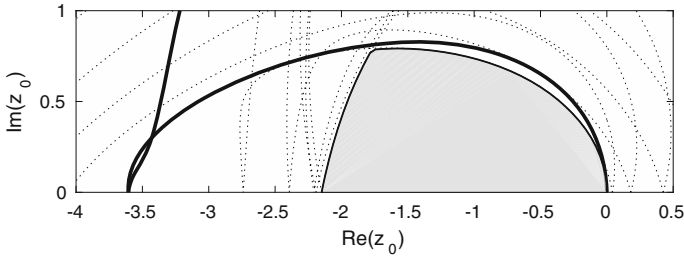


**Fig. 3** Stability region  $\mathcal{S}_E$  (thick line),  $\mathcal{S}_{\pi/2, y}$  for  $y = -2.0, -1.6, \dots, 2.0$  (thin dotted lines), and stability region  $\mathcal{S}_{\pi/2}$  (shaded region), of the IMEX GLM corresponding to (8.5)

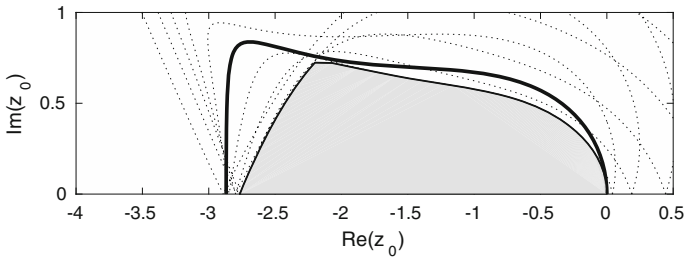


**Fig. 4** Stability region  $\mathcal{S}_E$  (thick line),  $\mathcal{S}_{\pi/2, y}$  for  $y = -2.0, -1.6, \dots, 2.0$  (thin dotted lines), and stability region  $\mathcal{S}_{\pi/2}$  (shaded region), of the IMEX GLM corresponding to (8.6)

for  $y = -2.0, -1.6, \dots, 2.0$  (thin dotted lines), and stability region  $\mathcal{S}_{\pi/2}$  (shaded region), of the IMEX GLM corresponding to (8.5).

Solving instead of (8.1) the minimization problem (8.2) corresponding to  $\alpha = \pi/2$  we get

$$\begin{aligned} \alpha_{12} &= -0.3131623044071503, & \alpha_{22} &= -0.0990668397968741, \\ \beta_{21} &= 0.7806559944423810, \end{aligned} \tag{8.6}$$

and for the corresponding IMEX GLM we have that  $\text{area}(\mathcal{S}_E \cap \mathbb{C}^-) = 3.73$ ,  $\text{area}(\mathcal{S}_{\pi/2} \cap \mathbb{C}^-) = 2.85$ . We have plotted on Fig. 4 stability region  $\mathcal{S}_E$  (thick line), stability regions  $\mathcal{S}_{\pi/2, y}$  for  $y = -2.0, -1.6, \dots, 2.0$  (thin dotted lines), and stability region  $\mathcal{S}_{\pi/2}$  (shaded region), of the IMEX GLM corresponding to (8.6).

### 8.2 IMEX GLMs with $p = q = 2$ and $r = s = 3$

Choosing  $\mathbf{c} = [0, 1/2, 1]^T$ ,  $\lambda = 1/4$ ,  $\epsilon = 0$ , and applying the algorithm described in Sect. 4 lead to the family of  $A$ - and  $L$ -stable GLMs with error constant  $E = -7/192$ , and coefficients depending on three free parameters  $\beta_1, \beta_2$ , and  $l_{21}$ . These coefficients are not listed here, but can be easily computed by symbolic manipulation packages following the algorithm described in Sect. 4.

As in Sect. 8.1 we will search next for IMEX GLMs with maximal area of  $\mathcal{S}_E \cap \mathbb{C}^-$  and  $\mathcal{S}_\alpha \cap \mathbb{C}^-$  for  $\alpha = \pi/2$ . Computing the first two columns  $\tilde{\alpha}$  of the matrix  $\alpha$  from the formula (6.4) we obtain a family of methods depending on free parameters  $\alpha_{13}, \alpha_{23}, \alpha_{33}, \beta_{21}, \beta_{31}$ , and  $\beta_{32}$ . Then solving the minimization problem (8.1) with respect to  $\alpha_{13}, \alpha_{23}, \alpha_{33}, \beta_{21}, \beta_{31}$ ,

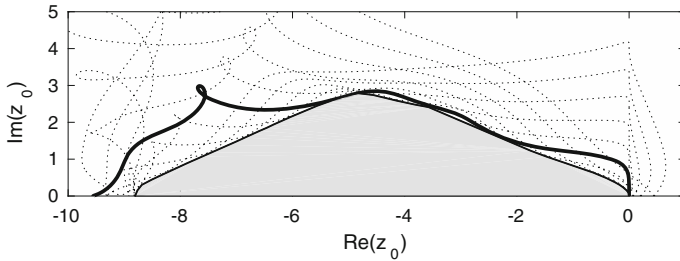


**Fig. 5** Stability region  $\mathcal{S}_E$  (thick line),  $\mathcal{S}_{\pi/2, y}$  for  $y = -4.0, -3.2, \dots, 4.0$  (thin dotted lines), and stability region  $\mathcal{S}_{\pi/2}$  (shaded region), of the IMEX GLM corresponding to (8.7)

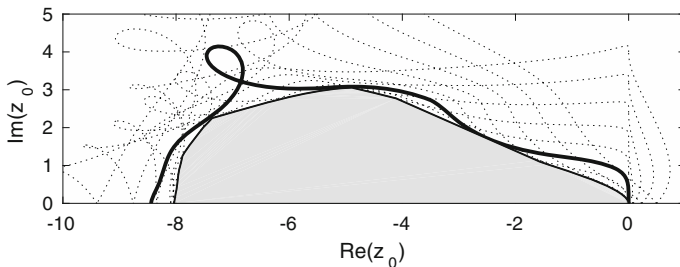


**Fig. 6** Stability region  $\mathcal{S}_E$  (thick line),  $\mathcal{S}_{\pi/2, y}$  for  $y = -4.0, -3.2, \dots, 4.0$  (thin dotted lines), and stability region  $\mathcal{S}_{\pi/2}$  (shaded region), of the IMEX GLM corresponding to (8.8)

$\beta_{32}, l_{21}, \beta_1,$  and  $\beta_2,$  we get

$$\begin{aligned}
 \alpha_{13} &= 0.7048042971366435, & \alpha_{23} &= 0.5806806426136659, \\
 \alpha_{33} &= -0.2480689169035659, & \beta_{21} &= 1.0070563539839243, \\
 \beta_{31} &= -0.7468987663950980 & \beta_{32} &= 1.8201469888045814, \\
 l_{21} &= 0.3204975065570276 & \beta_1 &= 0.1122368078518682, \\
 \beta_2 &= 0.0608031068496574, & &
 \end{aligned}
 \tag{8.7}$$

and for the corresponding IMEX GLM we have  $\text{area}(\mathcal{S}_E \cap \mathbb{C}^-) = 36.08,$   $\text{area}(\mathcal{S}_{\pi/2} \cap \mathbb{C}^-) = 27.77.$  We have plotted on Fig. 5 stability region  $\mathcal{S}_E$  (thick line), stability regions  $\mathcal{S}_{\pi/2, y}$  for  $y = -4.0, -3.2, \dots, 4.0$  (thin dotted lines), and stability region  $\mathcal{S}_{\pi/2}$  (shaded region), of the IMEX GLM corresponding to (8.7).

Solving instead of (8.1) the minimization problem (8.2) corresponding to  $\alpha = \pi/2$  we get

$$\begin{aligned}
 \alpha_{13} &= 0.7365201743639271, & \alpha_{23} &= 0.5352066674285787, \\
 \alpha_{33} &= -0.0912227599822747, & \beta_{21} &= 1.0209644666461690, \\
 \beta_{31} &= -0.7823766493497686, & \beta_{32} &= 1.6883120173647104, \\
 l_{21} &= 0.3253104517275260, & \beta_1 &= 0.0972139372675385, \\
 \beta_2 &= 0.0527904208800748, & &
 \end{aligned}
 \tag{8.8}$$

and for the corresponding IMEX GLM we have  $\text{area}(\mathcal{S}_E \cap \mathbb{C}^-) = 35.70,$   $\text{area}(\mathcal{S}_{\pi/2} \cap \mathbb{C}^-) = 31.59.$  We have plotted on Fig. 6 stability region  $\mathcal{S}_E$  (thick line), stability regions  $\mathcal{S}_{\pi/2, y}$  for  $y = -4.0, -3.2, \dots, 4.0$  (thin dotted lines), and stability region  $\mathcal{S}_{\pi/2}$  (shaded region), of the IMEX GLM corresponding to (8.8).

We will assume next that  $\beta_1 = \beta_2 = E = -7/192$ , and as in Sect. 8.1 we will search for IMEX GLMs with maximal area of  $\mathcal{S}_E \cap \mathbb{C}^-$  and  $\mathcal{S}_\alpha \cap \mathbb{C}^-$  for  $\alpha = \pi/2$ . Solving the minimization problem (8.1) with respect to  $\alpha_{13}, \alpha_{23}, \alpha_{33}, \beta_{21}, \beta_{31}, \beta_{32}$ , and  $l_{21}$  we get

$$\begin{aligned} \alpha_{13} &= -0.2761705959660553, & \alpha_{23} &= 1.5886193139724432, \\ \alpha_{33} &= 0.1251863223310433, & \beta_{21} &= -0.8470086913853645, \\ \beta_{31} &= -1.1165856084162047, & \beta_{32} &= 1.5757303345776144, \\ l_{21} &= -2.0616511332383398, \end{aligned} \tag{8.9}$$

and for the corresponding IMEX GLM we have  $\text{area}(\mathcal{S}_E \cap \mathbb{C}^-) = 22.33$ ,  $\text{area}(\mathcal{S}_{\pi/2} \cap \mathbb{C}^-) = 5.13$ . We have plotted on Fig. 7 stability region  $\mathcal{S}_E$  (thick line), stability regions  $\mathcal{S}_{\pi/2,y}$  for  $y = -4.0, -3.2, \dots, 4.0$  (thin dotted lines), and stability region  $\mathcal{S}_{\pi/2}$  (shaded region), of the IMEX GLM corresponding to (8.9).

Solving the minimization problem (8.2) corresponding to  $\alpha = \pi/2$  we get

$$\begin{aligned} \alpha_{13} &= -0.3359165568300500, & \alpha_{23} &= 1.7118797473647751, \\ \alpha_{33} &= 0.3698211954156955, & \beta_{21} &= -0.8849999789847105, \\ \beta_{31} &= -1.1404848830521810, & \beta_{32} &= 1.5218149707234159, \\ l_{21} &= -2.0838579492368345, \end{aligned} \tag{8.10}$$

and for the corresponding IMEX GLM we have  $\text{area}(\mathcal{S}_E \cap \mathbb{C}^-) = 24.29$ ,  $\text{area}(\mathcal{S}_{\pi/2} \cap \mathbb{C}^-) = 22.60$ . We have plotted on Fig. 8 stability region  $\mathcal{S}_E$  (thick line), stability regions  $\mathcal{S}_{\pi/2,y}$  for  $y = -4.0, -3.2, \dots, 4.0$  (thin dotted lines), and stability region  $\mathcal{S}_{\pi/2}$  (shaded region), of the IMEX GLM corresponding to (8.10).

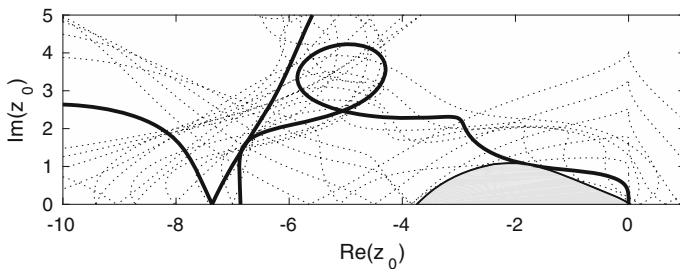


**Fig. 7** Stability region  $\mathcal{S}_E$  (thick line),  $\mathcal{S}_{\pi/2,y}$  for  $y = -4.0, -3.2, \dots, 4.0$  (thin dotted lines), and stability region  $\mathcal{S}_{\pi/2}$  (shaded region), of the IMEX GLM corresponding to (8.9)

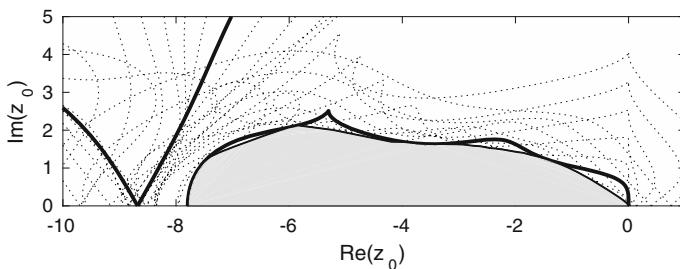


**Fig. 8** Stability region  $\mathcal{S}_E$  (thick line),  $\mathcal{S}_{\pi/2,y}$  for  $y = -4.0, -3.2, \dots, 4.0$  (thin dotted lines), and stability region  $\mathcal{S}_{\pi/2}$  (shaded region), of the IMEX GLM corresponding to (8.10)

### 8.3 IMEX GLMs with $p = q = 3$ and $r = s = 4$

Choosing  $\mathbf{c} = [0, 1/3, 2/3, 1]^T$ ,  $\lambda = 1/4$ ,  $\epsilon = 0$ , and applying the algorithm described in Sect. 4 lead to the family of  $A$ - and  $L$ -stable GLMs with error constant  $E = 1/256$ , and coefficients depending on six free parameters  $\beta_1, \beta_2, \beta_3, l_{21}, l_{31}$  and  $l_{32}$ . These coefficients are not listed here, but can be easily computed by symbolic manipulation packages following the algorithm described in Sect. 4.

As in previous sections we will search next for IMEX GLMs with maximal area of  $S_E \cap \mathbb{C}^-$  and  $S_\alpha \cap \mathbb{C}^-$  for  $\alpha = \pi/2$ . Computing the first three columns  $\tilde{\alpha}$  of the matrix  $\alpha$  from the formula (6.4) we obtain a family of methods depending on free parameters  $\alpha_{14}, \alpha_{24}, \alpha_{34}, \alpha_{44}, \beta_{21}, \beta_{31}, \beta_{32}, \beta_{41}, \beta_{42}$ , and  $\beta_{43}$ . Then solving the minimization problem (8.1) with respect to  $\alpha_{14}, \alpha_{24}, \alpha_{34}, \alpha_{44}, \beta_{21}, \beta_{31}, \beta_{32}, \beta_{41}, \beta_{42}, \beta_{43}, l_{21}, l_{31}, l_{32}, \beta_1, \beta_2$ , and  $\beta_3$ , we get

$$\begin{aligned}
 \alpha_{14} &= -0.0322061844618044, & \alpha_{24} &= -0.1371553807868855, \\
 \alpha_{34} &= -0.0475154208159705, & \alpha_{44} &= -0.4003970342611661, \\
 \beta_{21} &= 0.0340371060074856, & \beta_{31} &= -0.0105401588456497, \\
 \beta_{32} &= 0.6841861506702123, & \beta_{41} &= 0.7866040977985557, \\
 \beta_{42} &= 0.4197043822869505, & \beta_{43} &= -0.2629538237615239, \\
 l_{21} &= 0.9749809251405265, & l_{31} &= 0.0340619859556146 \\
 l_{32} &= -0.2435531549748590, & \beta_1 &= 0.7634506787898878, \\
 \beta_2 &= 0.3094061851203284, & \beta_3 &= 0.0574266399871909,
 \end{aligned}
 \tag{8.11}$$

and for the corresponding IMEX GLM we have that  $\text{area}(S_E \cap \mathbb{C}^-) = 6.08$ ,  $\text{area}(S_{\pi/2} \cap \mathbb{C}^-) = 0.44$ . We have plotted on Fig. 9 stability region  $S_E$  (thick line), stability regions  $S_{\pi/2, y}$  for  $y = -6.0, -4.8, \dots, 6.0$  (thin dotted lines), and stability region  $S_{\pi/2}$  (shaded region), of the IMEX GLM corresponding to (8.11).

Solving instead of (8.1) the minimization problem (8.2) corresponding to  $\alpha = \pi/2$  we get

$$\begin{aligned}
 \alpha_{14} &= -0.0019343661189984, & \alpha_{24} &= -0.1002080612577962, \\
 \alpha_{34} &= -0.1776066045171551, & \alpha_{44} &= -0.0245141224985896, \\
 \beta_{21} &= 0.6059088353566069, & \beta_{31} &= -0.4194105236466259, \\
 \beta_{32} &= 0.9333216543167162, & \beta_{41} &= 0.5003134666349642, \\
 \beta_{42} &= 0.5364733937398944, & \beta_{43} &= 0.0414877738155996, \\
 l_{21} &= -0.6952599952291396, & l_{31} &= 2.5437820700922353, \\
 l_{32} &= -0.0234149225419190, & \beta_1 &= 0.2419090231319946, \\
 \beta_2 &= 0.0685000212896784, & \beta_3 &= -0.0607397082621161,
 \end{aligned}
 \tag{8.12}$$

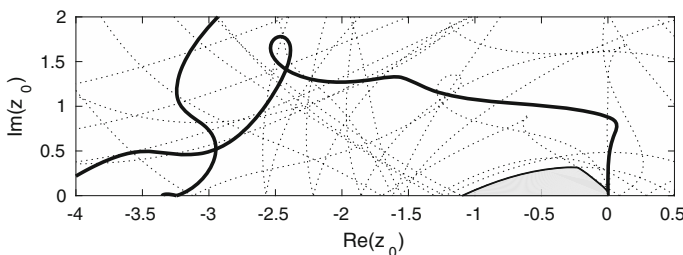


**Fig. 9** Stability region  $S_E$  (thick line),  $S_{\pi/2, y}$  for  $y = -6.0, -4.8, \dots, 6.0$  (thin dotted lines), and stability region  $S_{\pi/2}$  (shaded region), of the IMEX GLM corresponding to (8.11)

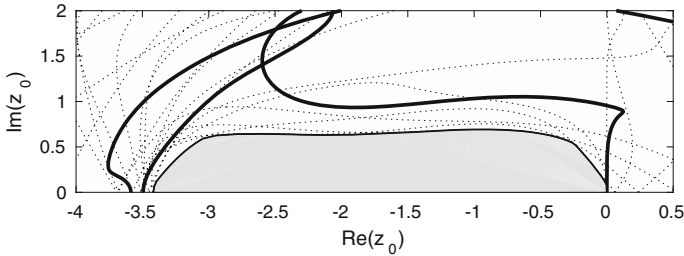


**Fig. 10** Stability region  $S_E$  (thick line),  $S_{\pi/2,y}$  for  $y = -6.0, -4.8, \dots, 6.0$  (thin dotted lines), and stability region  $S_{\pi/2}$  (shaded region), of the IMEX GLM corresponding to (8.12)

and for the corresponding IMEX GLM we have that  $\text{area}(S_E \cap \mathbb{C}^-) = 5.85$ ,  $\text{area}(S_{\pi/2} \cap \mathbb{C}^-) = 3.97$ . We have plotted on Fig. 10 stability region  $S_E$  (thick line), stability regions  $S_{\pi/2,y}$  for  $y = -6.0, -4.8, \dots, 6.0$  (thin dotted lines), and stability region  $S_{\pi/2}$  (shaded region), of the IMEX GLM corresponding to (8.12).

We will assume next that  $\beta_1 = \beta_2 = \beta_3 = E = 1/256$ , and as in previous sections we will search for IMEX GLMs with maximal area of  $S_E \cap \mathbb{C}^-$  and  $S_\alpha \cap \mathbb{C}^-$  for  $\alpha = \pi/2$ . Solving the minimization problem (8.1) with respect to  $\alpha_{14}, \alpha_{24}, \alpha_{34}, \alpha_{44}, \beta_{21}, \beta_{31}, \beta_{32}, \beta_{41}, \beta_{42}, \beta_{43}, l_{21}, l_{31}$ , and  $l_{32}$  we get

$$\begin{aligned}
 \alpha_{14} &= 2.4913016363912952, & \alpha_{24} &= -0.3263777127054882, \\
 \alpha_{34} &= -0.0337355771614116, & \alpha_{44} &= -0.1960110025688487, \\
 \beta_{21} &= -0.3357508741005324, & \beta_{31} &= -0.5501933294865551, \\
 \beta_{32} &= 0.6562982997350197, & \beta_{41} &= -0.0599065394156352, \\
 \beta_{42} &= -0.3575046987978234, & \beta_{43} &= 1.2793832728383250, \\
 l_{21} &= -1.2579071563931954, & l_{31} &= 1.3920885377139143, \\
 l_{32} &= -3.6453949643924055, & &
 \end{aligned}
 \tag{8.13}$$

and for the corresponding IMEX GLM we have that  $\text{area}(S_E \cap \mathbb{C}^-) = 1.50$ ,  $\text{area}(S_{\pi/2} \cap \mathbb{C}^-) = 0.41$ . We have plotted on Fig. 11 stability region  $S_E$  (thick line), stability regions  $S_{\pi/2,y}$  for  $y = -6.0, -4.8, \dots, 6.0$  (thin dotted lines), and stability region  $S_{\pi/2}$  (shaded region), of the IMEX GLM corresponding to (8.13).

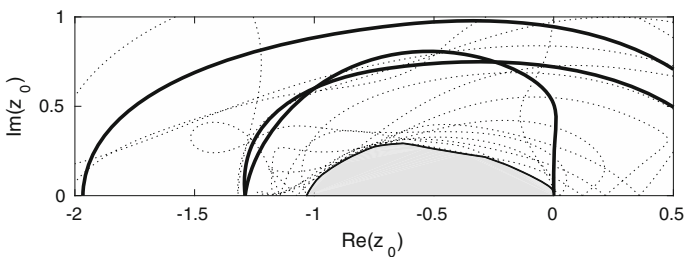


**Fig. 11** Stability region  $S_E$  (thick line),  $S_{\pi/2,y}$  for  $y = -6.0, -4.8, \dots, 6.0$  (thin dotted lines), and stability region  $S_{\pi/2}$  (shaded region), of the IMEX GLM corresponding to (8.13)

Solving the minimization problem (8.2) corresponding to  $\alpha = \pi/2$  we get

$$\begin{aligned}
 \alpha_{14} &= 1.5424196324308657, & \alpha_{24} &= -4.1167439198814524, \\
 \alpha_{34} &= -1.6702155839518298, & \alpha_{44} &= -1.1675407400567321, \\
 \beta_{21} &= -1.6179065072363725, & \beta_{31} &= -1.5992858415405253, \\
 \beta_{32} &= 0.1496219631792377, & \beta_{41} &= 0.2487036951180054, \\
 \beta_{42} &= -1.3275472729892113, & \beta_{43} &= 1.7236437628213972, \\
 l_{21} &= -1.1601015500948186, & l_{31} &= -0.9375050588633353, \\
 l_{32} &= -0.0640870397984420, & &
 \end{aligned}
 \tag{8.14}$$

and for the corresponding IMEX GLM we have that  $\text{area}(S_E \cap \mathbb{C}^-) = 1.06$ ,  $\text{area}(S_{\pi/2} \cap \mathbb{C}^-) = 0.48$ . We have plotted on Fig. 12 stability region  $S_E$  (thick line), stability regions  $S_{\pi/2, y}$  for  $y = -6.0, -4.8, \dots, 6.0$  (thin dotted lines), and stability region  $S_{\pi/2}$  (shaded region), of the IMEX GLM corresponding to (8.14).

### 8.4 IMEX GLMs with $p = q = 4$ and $r = s = 5$

Choosing  $\mathbf{c} = [0, 1/4, 1/2, 3/4, 1]^T$ ,  $\lambda = 1/2$ ,  $\epsilon = 0$ , and applying the algorithm described in Sect. 4 lead to the family of  $A$ - and  $L$ -stable GLMs with error constant  $E = -11/480$ , (there is a misprint in [33] where the error constant  $E = -11/48$  was reported), and coefficients depending on ten free parameters  $\beta_1, \beta_2, \beta_3, \beta_4, l_{21}, l_{31}, l_{32}, l_{41}, l_{42}$ , and  $l_{43}$ . These coefficients are not listed here, but can be easily computed by symbolic manipulation packages following the algorithm described in Sect. 4.

As in previous sections we will search next for IMEX GLMs with maximal area of  $S_E \cap \mathbb{C}^-$  and  $S_\alpha \cap \mathbb{C}^-$  for  $\alpha = \pi/2$ . Computing the first four columns  $\tilde{\alpha}$  of the matrix  $\alpha$  from the formula (6.4), and then computing the coefficient matrices  $\bar{\mathbf{A}}, \mathbf{A}^*, \bar{\mathbf{B}}$ , and  $\mathbf{B}^*$  from (5.3) we obtain a family of IMEX schemes depending on free parameters  $\alpha_{15}, \alpha_{25}, \alpha_{35}, \alpha_{45}, \alpha_{55}, \beta_{21}, \beta_{31}, \beta_{32}, \beta_{41}, \beta_{42}, \beta_{43}, \beta_{51}, \beta_{52}, \beta_{53}, \beta_{54}, \beta_1, \beta_2, \beta_3, \beta_4, l_{21}, l_{31}, l_{32}, l_{41}, l_{42}$ , and  $l_{43}$ . Then solving the minimization problem (8.1) with respect to these parameters we get

$$\begin{aligned}
 \alpha_{15} &= 0.0923741849195715, & \alpha_{25} &= 0.0028604913471628, \\
 \alpha_{35} &= -0.0279944894113296, & \alpha_{45} &= 0.0744140295424507, \\
 \alpha_{55} &= -0.8876038729025343, & \beta_{21} &= 0.3434117281181724, \\
 \beta_{31} &= 0.3184480901895457, & \beta_{32} &= 0.4437862773506412, \\
 \beta_{41} &= 0.0237584066604190, & \beta_{42} &= 0.8704911982416659, \\
 \beta_{43} &= 0.2673995304638158, & \beta_{51} &= -0.1482175175698811, \\
 \beta_{52} &= 5.3309724955200162, & \beta_{53} &= -0.7134521837118601, \\
 \beta_{54} &= -0.5317915290823025, & l_{21} &= -0.8161576100361232, \\
 l_{31} &= -0.5420772764208202, & l_{32} &= 0.1698222174580972, \\
 l_{41} &= 0.3086160843412334, & l_{42} &= -0.0142677947828854, \\
 l_{43} &= 0.3818368601311756, & \beta_1 &= 0.2293632290779495, \\
 \beta_2 &= -0.5819713279357461, & \beta_3 &= -0.1079195809643189, \\
 \beta_4 &= 0.1390683810799995, & &
 \end{aligned}
 \tag{8.15}$$

and for the corresponding IMEX GLM we have that  $\text{area}(S_E \cap \mathbb{C}^-) = 2.08$ ,  $\text{area}(S_{\pi/2} \cap \mathbb{C}^-) = 0.31$ . We have plotted on Fig. 13 stability region  $S_E$  (thick line), stability regions  $S_{\pi/2, y}$

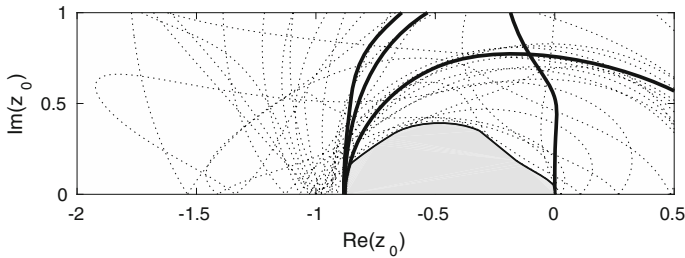


**Fig. 12** Stability region  $\mathcal{S}_E$  (thick line),  $\mathcal{S}_{\pi/2,y}$  for  $y = -6.0, -4.8, \dots, 6.0$  (thin dotted lines), and stability region  $\mathcal{S}_{\pi/2}$  (shaded region), of the IMEX GLM corresponding to (8.14)

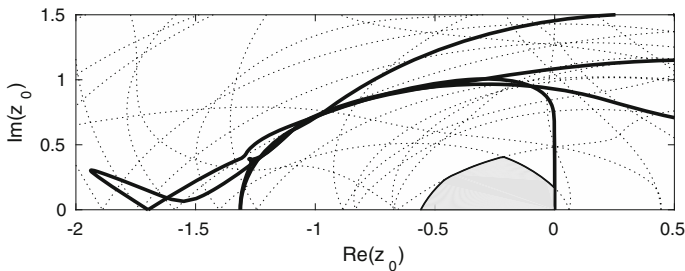


**Fig. 13** Stability region  $\mathcal{S}_E$  (thick line),  $\mathcal{S}_{\pi/2,y}$  for  $y = -8.0, -6.4, \dots, 8.0$  (thin dotted lines), and stability region  $\mathcal{S}_{\pi/2}$  (shaded region), of the IMEX GLM corresponding to (8.15)

for  $y = -8.0, -6.4, \dots, 8.0$  (thin dotted lines), and stability region  $\mathcal{S}_{\pi/2}$  (shaded region), of the IMEX GLM corresponding to (8.15).

Solving instead of (8.1) the minimization problem (8.2) corresponding to  $\alpha = \pi/2$  we get

$$\begin{aligned}
 \alpha_{15} &= -1.2114571208369744, & \alpha_{25} &= 0.0884241105232028, \\
 \alpha_{35} &= 0.8467139943266520, & \alpha_{45} &= 0.9534329964232042, \\
 \alpha_{55} &= 2.3902208001689269, & \beta_{21} &= -1.1297348700159846, \\
 \beta_{31} &= -1.2988168436128529, & \beta_{32} &= 0.6205202797503988, \\
 \beta_{41} &= -0.2206138517333536, & \beta_{42} &= 0.7496647677233477, \\
 \beta_{43} &= 0.5455160580650258, & \beta_{51} &= -0.5264456434481564, \\
 \beta_{52} &= 0.1844183845443656, & \beta_{53} &= 1.2264032883145131, \\
 \beta_{54} &= 0.0535874163121930, & l_{21} &= 0.0272112145389444, \\
 l_{31} &= 0.8885922249897176, & l_{32} &= 2.1709933522310738, \\
 l_{41} &= -2.6275666492736693, & l_{42} &= 1.8497574700032668, \\
 l_{43} &= 0.2768774661581863, & \beta_1 &= 0.3104914332552080, \\
 \beta_2 &= -0.3072308116407267, & \beta_3 &= -0.2380997038887391, \\
 \beta_4 &= 0.1045726706019693, & & 
 \end{aligned}
 \tag{8.16}$$

and for the corresponding IMEX GLM we have that  $\text{area}(\mathcal{S}_E \cap \mathbb{C}^-) = 1.04$ ,  $\text{area}(\mathcal{S}_{\pi/2} \cap \mathbb{C}^-) = 0.84$ . We have plotted on Fig. 14 stability region  $\mathcal{S}_E$  (thick line), stability regions  $\mathcal{S}_{\pi/2,y}$  for  $y = -8.0, -6.4, \dots, 8.0$  (thin dotted lines), and stability region  $\mathcal{S}_{\pi/2}$  (shaded region), of the IMEX GLM corresponding to (8.16).

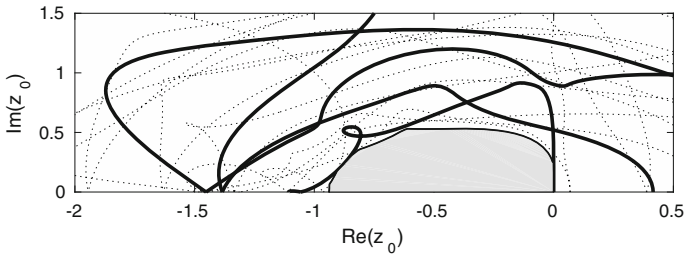


**Fig. 14** Stability region  $\mathcal{S}_E$  (thick line),  $\mathcal{S}_{\pi/2,y}$  for  $y = -8.0, -6.4, \dots, 8.0$  (thin dotted lines), and stability region  $\mathcal{S}_{\pi/2}$  (shaded region), of the IMEX GLM corresponding to (8.16)

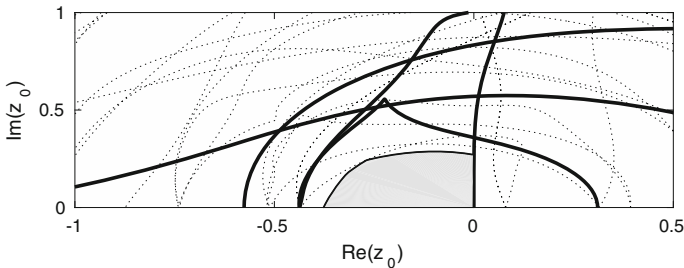


**Fig. 15** Stability region  $\mathcal{S}_E$  (thick line),  $\mathcal{S}_{\pi/2,y}$  for  $y = -8.0, -6.4, \dots, 8.0$  (thin dotted lines), and stability region  $\mathcal{S}_{\pi/2}$  (shaded region), of the IMEX GLM corresponding to (8.17)

We will assume next that  $\beta_1 = \beta_2 = \beta_3 = \beta_4 = E = -11/480$ , and as in previous sections we will search for IMEX GLMs with maximal area of  $\mathcal{S}_E \cap \mathbb{C}^-$  and  $\mathcal{S}_\alpha \cap \mathbb{C}^-$  for  $\alpha = \pi/2$ . Solving the minimization problem (8.1) with respect to  $\alpha_{15}, \alpha_{25}, \alpha_{35}, \alpha_{45}, \alpha_{55}, \beta_{21}, \beta_{31}, \beta_{32}, \beta_{41}, \beta_{42}, \beta_{43}, \beta_{51}, \beta_{52}, \beta_{53}, \beta_{54}, l_{21}, l_{31}, l_{32}, l_{41}, l_{42},$  and  $l_{43}$ , we get

$$\begin{aligned}
 \alpha_{15} &= -0.4274525221028934, & \alpha_{25} &= -0.2582571710558640, \\
 \alpha_{35} &= -0.1291872683142936, & \alpha_{45} &= -0.3299694472868494, \\
 \alpha_{55} &= -0.0737098285813478, & \beta_{21} &= 0.2180451276692885, \\
 \beta_{31} &= 0.5039672089986353, & \beta_{32} &= -0.1119314668217859, \\
 \beta_{41} &= 0.4010004394225283, & \beta_{42} &= 0.2028234562476922, \\
 \beta_{43} &= -0.2229723433280797, & \beta_{51} &= 0.5824815163627148, \\
 \beta_{52} &= -0.8592788525419057, & \beta_{53} &= 0.4355708332749956, \\
 \beta_{54} &= -0.0745288186133695, & l_{21} &= -0.2563143235341758, \\
 l_{31} &= 0.0451848220006013, & l_{32} &= -0.7423539897154100, \\
 l_{41} &= 0.1894838040143801, & l_{42} &= -1.9589403098423417, \\
 l_{43} &= -3.7612248865480944, & &
 \end{aligned}
 \tag{8.17}$$

and for the corresponding IMEX GLM we have that  $\text{area}(\mathcal{S}_E \cap \mathbb{C}^-) = 0.34$ ,  $\text{area}(\mathcal{S}_{\pi/2} \cap \mathbb{C}^-) = 0.18$ . We have plotted on Fig. 15 stability region  $\mathcal{S}_E$  (thick line), stability regions  $\mathcal{S}_{\pi/2,y}$  for  $y = -8.0, -6.4, \dots, 8.0$  (thin dotted lines), and stability region  $\mathcal{S}_{\pi/2}$  (shaded region), of the IMEX GLM corresponding to (8.17).



Solving the minimization problem (8.2) corresponding to  $\alpha = \pi/2$  we get

$$\begin{aligned}
 \alpha_{15} &= -0.4166609648529102, & \alpha_{25} &= -0.2613010013324336, \\
 \alpha_{35} &= -0.1278859963954986, & \alpha_{45} &= -0.3290333912717879, \\
 \alpha_{55} &= -0.0734594546946313, & \beta_{21} &= 0.2187775334418260, \\
 \beta_{31} &= 0.5037687681777114, & \beta_{32} &= -0.1120670630938067, \\
 \beta_{41} &= 0.4014719362836769, & \beta_{42} &= 0.2031160072843976, \\
 \beta_{43} &= -0.2228262082299665, & \beta_{51} &= 0.5816599966564926, \\
 \beta_{52} &= -0.8584475361360557, & \beta_{53} &= 0.4358509993886504, \\
 \beta_{54} &= -0.0743512326250040, & l_{21} &= -0.2500327894252148, \\
 l_{31} &= 0.0450118523274493, & l_{32} &= -0.7491539813690300, \\
 l_{41} &= 0.1883635069360757, & l_{42} &= -1.9865695985325744, \\
 l_{43} &= -3.7498849269761640,
 \end{aligned}
 \tag{8.18}$$

and for the corresponding IMEX GLM we have that  $\text{area}(\mathcal{S}_E \cap \mathbb{C}^-) = 0.27$ ,  $\text{area}(\mathcal{S}_{\pi/2} \cap \mathbb{C}^-) = 0.24$ . We have plotted on Fig. 16 stability region  $\mathcal{S}_E$  (thick line), stability regions  $\mathcal{S}_{\pi/2,y}$  for  $y = -8.0, -6.4, \dots, 8.0$  (thin dotted lines), and stability region  $\mathcal{S}_{\pi/2}$  (shaded region), of the IMEX GLM corresponding to (8.18).

### 8.5 Comparison of IMEX GLMs with IRKS with Other Classes of Extrapolated IMEX Methods

In this section we compare areas of stability regions  $\mathcal{S}_E \cap \mathbb{C}^-$  and  $\mathcal{S}_{\pi/2} \cap \mathbb{C}^-$  of extrapolated IMEX GLMs with IRKS investigated in this paper with the corresponding areas of extrapolated IMEX DIMSIMs investigated in [19,20] and extrapolated IMEX SDIRK methods investigated in [21]. The areas of  $\mathcal{S}_E \cap \mathbb{C}^-$  and  $\mathcal{S}_{\pi/2} \cap \mathbb{C}^-$  of extrapolated IMEX DIMSIMs constructed in [19,20] are listed in Table 1 and the corresponding areas of extrapolated IMEX SDIRK methods constructed in [21] are listed in Table 2. The areas of  $\mathcal{S}_E \cap \mathbb{C}^-$  and  $\mathcal{S}_{\pi/2} \cap \mathbb{C}^-$  of the IMEX GLMs with IRKS are listed in Table 3 for methods where the parameters  $\beta_1, \beta_2, \dots, \beta_s$  were used to maximize the area of stability of the explicit GLM or of the IMEX scheme assuming that the implicit part of the method is  $A$ -stable, and in Table 4 for methods with  $\beta_1 = \beta_2 = \dots = \beta_s = E$  (compare Sect. 4).

We can observe that IMEX GLMs with IRKS, where the free parameters  $\beta_1, \beta_2, \dots, \beta_s$  were used to maximize the region of stability of explicit part of the method assuming that the implicit part is  $A$ -stable, have with one exception, larger areas of  $\mathcal{S}_E \cap \mathbb{C}^-$  and  $\mathcal{S}_{\pi/2} \cap \mathbb{C}^-$  than the extrapolated IMEX DIMSIMs constructed in [19,20] and extrapolated IMEX SDIRK methods for  $p = s = 1$  and  $p = s = 2$ . These areas are smaller as compared with IMEX

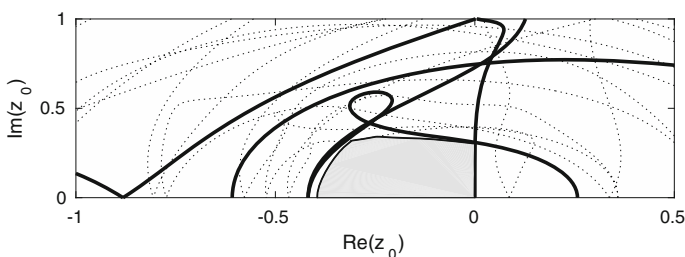


**Fig. 16** Stability region  $\mathcal{S}_E$  (thick line),  $\mathcal{S}_{\pi/2,y}$  for  $y = -8.0, -6.4, \dots, 8.0$  (thin dotted lines), and stability region  $\mathcal{S}_{\pi/2}$  (shaded region), of the IMEX GLM corresponding to (8.18)

SDIRK methods for  $p = s = 3$  and  $s = 5, p = 4$ . However, all methods constructed in this paper have stage order  $q$  equal to the order  $p$ , and contrary to IMEX SDIRK methods which have low stage order, they do not suffer from order reduction phenomenon when applied to stiff differential systems.

The better stability properties of the IMEX GLMs constructed in this paper do not come for free. The new schemes take one additional internal stage and one additional external stage as compared to the extrapolated DIMSIMs constructed in [19,20].

### 9 Numerical Experiments

The IMEX GLMs with IRKS constructed in this paper have order  $p$  and stage order  $q = p$  and, as a result, they do not suffer from order reduction phenomenon which affects, for example, some classes of IMEX RK methods [5,28,35,38,39]. IMEX RK methods of third order which do not suffer from order reduction were constructed in [6,8].

A useful test problem to investigate a possible order reduction of numerical schemes is the van der Pol equation

$$y' = \begin{bmatrix} y'_1 \\ y'_2 \end{bmatrix} = \underbrace{\begin{bmatrix} y_2 \\ 0 \end{bmatrix}}_{f(y)} + \underbrace{\begin{bmatrix} 0 \\ ((1 - y_1^2)y_2 - y_1) / \epsilon \end{bmatrix}}_{g(y)}, \tag{9.1}$$

which is splitted into the non-stiff part  $f(y)$  and the stiff part  $g(y)$  for  $0 < \epsilon \ll 1$ . As in [5,21,22] this system was integrated on the time interval  $[0, t_{end}]$  with  $t_{end} = 0.55139$ , and with initial values given by

$$y_1(0) = 2, \quad y_2(0) = -\frac{2}{3} + \frac{10}{81}\epsilon - \frac{292}{2187}\epsilon^2 - \frac{1814}{19683}\epsilon^3 + O(\epsilon^4).$$

**Table 1** Areas of  $S_E \cap \mathbb{C}^-$  and  $S_{\pi/2} \cap \mathbb{C}^-$  for extrapolated IMEX DIMSIMs investigated in [19,20]

$p=q=r=s$	$-\text{area}(S_E \cap \mathbb{C}^-) \rightarrow \min$		$-\text{area}(S_{\pi/2} \cap \mathbb{C}^-) \rightarrow \min$	
	$\text{area}(S_E \cap \mathbb{C}^-)$	$\text{area}(S_{\pi/2} \cap \mathbb{C}^-)$	$\text{area}(S_E \cap \mathbb{C}^-)$	$\text{area}(S_{\pi/2} \cap \mathbb{C}^-)$
1	4.27	3.98	4.21	4.03
2	7.15	5.74	7.14	5.75
3	3.54	0.39	1.04	0.50
4	2.82	0.0069	0.18	0.16

**Table 2** Areas of  $S_E \cap \mathbb{C}^-$  and  $S_{\pi/2} \cap \mathbb{C}^-$  for extrapolated IMEX SDIRK methods investigated in [21]

$p, s$	$-\text{area}(S_E \cap \mathbb{C}^-) \rightarrow \min$		$-\text{area}(S_{\pi/2} \cap \mathbb{C}^-) \rightarrow \min$	
	$\text{area}(S_E \cap \mathbb{C}^-)$	$\text{area}(S_{\pi/2} \cap \mathbb{C}^-)$	$\text{area}(S_E \cap \mathbb{C}^-)$	$\text{area}(S_{\pi/2} \cap \mathbb{C}^-)$
$p = s = 1$	4.27	3.98	4.21	4.03
$p = s = 2$	8.83	7.18	8.81	7.20
$p = s = 3$	14.19	5.00	13.42	10.65
$p = 4, s = 5$	2.82	1.06	2.47	1.50

**Table 3** Areas of  $\mathcal{S}_E \cap \mathbb{C}^-$  and  $\mathcal{S}_{\pi/2} \cap \mathbb{C}^-$  for extrapolated IMEX GLMs with IRKS, where the parameters  $\beta_1, \beta_2, \dots, \beta_s$  were used to maximize the area of stability of the explicit GLM or of the IMEX scheme assuming that the implicit part of the method is  $A$ -stable

$p, s$	$-\text{area}(\mathcal{S}_E \cap \mathbb{C}^-) \rightarrow \min$		$-\text{area}(\mathcal{S}_{\pi/2} \cap \mathbb{C}^-) \rightarrow \min$	
	$\text{area}(\mathcal{S}_E \cap \mathbb{C}^-)$	$\text{area}(\mathcal{S}_{\pi/2} \cap \mathbb{C}^-)$	$\text{area}(\mathcal{S}_E \cap \mathbb{C}^-)$	$\text{area}(\mathcal{S}_{\pi/2} \cap \mathbb{C}^-)$
$p = 1, s = 2$	24.45	16.49	21.75	19.19
$p = 2, s = 3$	36.08	27.77	35.70	31.59
$p = 3, s = 4$	6.08	0.44	5.85	3.97
$p = 4, s = 5$	2.08	0.31	1.04	0.84

**Table 4** Areas of  $\mathcal{S}_E \cap \mathbb{C}^-$  and  $\mathcal{S}_{\pi/2} \cap \mathbb{C}^-$  for extrapolated IMEX GLMs with IRKS, where  $\beta_1 = \beta_2 = \dots = \beta_s = E$

$p, s$	$-\text{area}(\mathcal{S}_E \cap \mathbb{C}^-) \rightarrow \min$		$-\text{area}(\mathcal{S}_{\pi/2} \cap \mathbb{C}^-) \rightarrow \min$	
	$\text{area}(\mathcal{S}_E \cap \mathbb{C}^-)$	$\text{area}(\mathcal{S}_{\pi/2} \cap \mathbb{C}^-)$	$\text{area}(\mathcal{S}_E \cap \mathbb{C}^-)$	$\text{area}(\mathcal{S}_{\pi/2} \cap \mathbb{C}^-)$
$p = 1, s = 2$	4.50	2.58	3.73	2.85
$p = 2, s = 3$	22.33	5.13	24.29	22.60
$p = 3, s = 4$	1.50	0.41	1.06	0.48
$p = 4, s = 5$	0.34	0.18	0.27	0.24

As discussed in [5, 36] for these initial values the system (9.1) is stiff for small values of  $\epsilon$  on the whole interval of integration  $[0, t_{end}]$  (there are no initial transients on which the problem is non-stiff). (Observe that in [28, 35–37, 50] this problem was integrated on the time interval  $[0, 0.5]$ ). Integrating (9.1) we treated the non-stiff part  $f(y)$  by the explicit method and the stiff part  $g(y)$  by the implicit method. The required starting values  $Y_i^{[1]} \approx y(t_0 + c_i h), i = 1, 2, \dots, s$ , were computed using the Matlab code `ode15s` with tolerances  $\text{AbsTol} = 10^{-14}$  and  $\text{RelTol} = 10^{-12}$ . We also need approximations to

$$y_i^{[1]} \approx h^{i-1} \begin{bmatrix} y_1^{(i-1)}(t_0 + h) \\ y_2^{(i-1)}(t_0 + h) \end{bmatrix}, \quad i = 1, 2, \dots, p + 1.$$

As in [16], putting  $y_i = y_1^{(i-1)} = y_2^{(i-2)}, i = 3, 4, \dots, p + 2, p = 1, 2, 3, 4$ , the successive derivatives of the vector function  $y = [y_1, y_2]^T$  are given by

$$y' = \begin{bmatrix} y_2 \\ y_3 \end{bmatrix}, \quad y'' = \begin{bmatrix} y_3 \\ y_4 \end{bmatrix}, \quad y''' = \begin{bmatrix} y_4 \\ y_5 \end{bmatrix}, \quad y^{(4)} = \begin{bmatrix} y_5 \\ y_6 \end{bmatrix},$$

where  $y_3, y_4, y_5$ , and  $y_6$ , can be computed from the recurrence relations

$$\begin{aligned} y_3 &= ((1 - y_1^2)y_2 - y_1) / \epsilon, \\ y_4 &= ((1 - y_1^2)y_3 - 2y_1y_2^2 - y_2) / \epsilon, \\ y_5 &= ((1 - y_1^2)y_4 - 6y_1y_2y_3 - 2y_2^3 - y_3) / \epsilon, \\ y_6 &= ((1 - y_1^2)y_5 - 8y_1y_2y_4 - 12y_2^2y_3 - 6y_1y_3^2 - y_4) / \epsilon. \end{aligned}$$

(Observe that there are some small misprints in [16]). To solve the nonlinear systems of equations with respect to  $Y_i^{[n+1]}$ , resulting from the application of IMEX schemes (5.2) to

(9.1), we have used the exact Jacobian of the function  $g(y)$  given by

$$J_g(y) = \frac{\partial g}{\partial y} = \begin{bmatrix} \frac{\partial g_1}{\partial y_1} & \frac{\partial g_1}{\partial y_2} \\ \frac{\partial g_2}{\partial y_1} & \frac{\partial g_2}{\partial y_2} \end{bmatrix} = \begin{bmatrix} 0 & 0 \\ \frac{-2y_1y_2 - 1}{\epsilon} & \frac{1 - y_1^2}{\epsilon} \end{bmatrix}.$$

The results of numerical experiments with IMEX schemes (8.4), (8.8), (8.12), and (8.16) are presented in Figs. 17, 18, 19, and 20. On these figures we have plotted in double logarithmic scale the norm of the error at the end of the interval of integration versus stepsize  $h$  for  $\epsilon = 10^{-1}$  and  $\epsilon = 10^{-6}$ , and the theoretical slope of convergence corresponding to the order of the method  $p$ ,  $p = 1, 2, 3, 4$ . Similar results were obtained for the other methods listed in Sect. 8. We can observe that all IMEX GLMs with IRKS achieve the expected order of accuracy, and that there is no order reduction for these methods. We have also listed in Table 5 the stepsizes  $h$ ,  $L_1$ -norm of errors at the endpoint  $t_{end}$ , the ratios  $\|error\|_1/h^4$ , and the observed order of accuracy  $p$  for the IMEX scheme (8.16) of order  $p = 4$  and stage order  $q = p = 4$ . The approximation to the reference solution  $y(t_{end}) = [y_1(t_{end}), y_2(t_{end})]^T$  was computed by Matlab code `ode15s` with  $AbsTol = 10^{-14}$  and  $RelTol = 10^{-12}$ .

Consider next the linear advection-reaction equation [19,20,29]

$$\begin{cases} \frac{\partial u}{\partial t} + \alpha_1 \frac{\partial u}{\partial x} = -k_1u + k_2v + s_1, \\ \frac{\partial v}{\partial t} + \alpha_2 \frac{\partial v}{\partial x} = k_1u - k_2v + s_2, \end{cases} \tag{9.2}$$

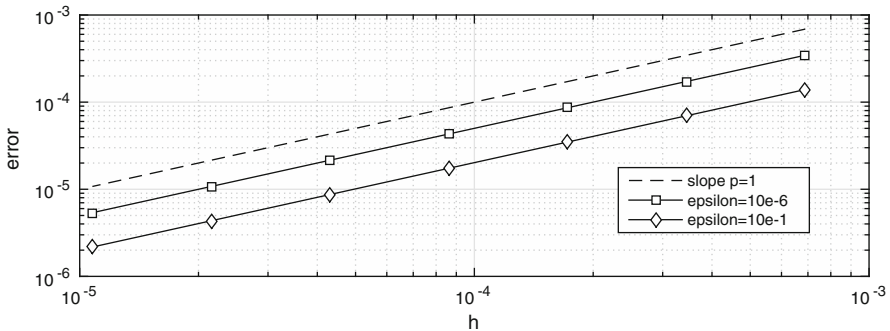


Fig. 17 Error versus stepsize for IMEX GLM with IRKS (8.4) of order  $p = 1$  and stage order  $q = p = 1$

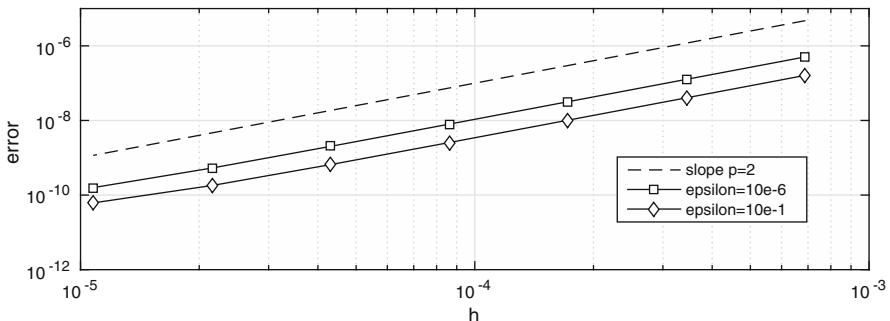
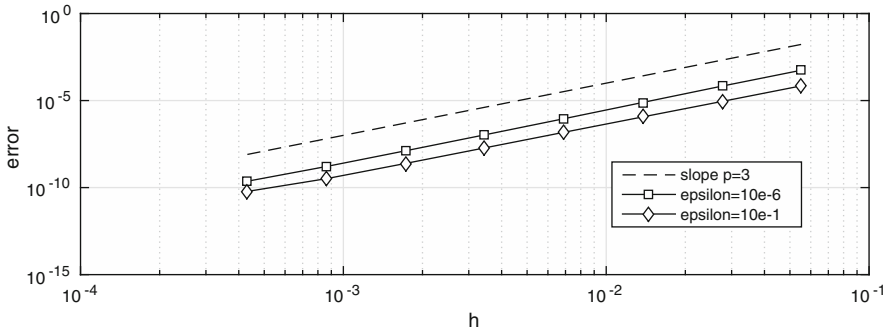
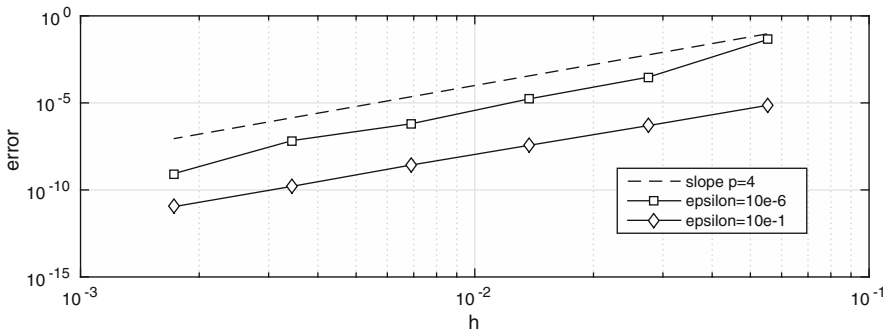


Fig. 18 Error versus stepsize for IMEX GLM with IRKS (8.8) of order  $p = 2$  and stage order  $q = p = 2$



**Fig. 19** Error versus stepsize for IMEX GLM with IRKS (8.12) of order  $p = 3$  and stage order  $q = p = 3$



**Fig. 20** Error versus stepsize for IMEX GLM with IRKS (8.16) of order  $p = 4$  and stage order  $q = p = 4$

**Table 5**  $L_1$ -norm of errors, ratios  $\|error\|_1/h^4$ , and observed orders of convergence  $p$  versus stepsize  $h$  for IMEX GLM with IRKS (8.16) applied to (9.1) with  $\epsilon = 10^{-1}$  and  $\epsilon = 10^{-6}$

$h$	$\ error\ _1$		$\ error\ _1/h^4$		$p$	
	$\epsilon = 10^{-1}$	$\epsilon = 10^{-6}$	$\epsilon = 10^{-1}$	$\epsilon = 10^{-6}$	$\epsilon = 10^{-1}$	$\epsilon = 10^{-6}$
5.51e-02	7.17e-06	4.28e-02	0.78	4633		
2.76e-02	4.97e-07	3.03e-04	0.86	524	3.85	7.14
1.39e-02	3.71e-08	1.73e-05	1.03	479	3.74	4.13
6.89e-03	2.69e-09	6.29e-07	1.19	279	3.79	4.78
3.45e-03	1.62e-10	6.88e-08	1.15	488	4.05	3.19
1.72e-03	1.09e-11	8.54e-10	1.24	96.9	3.90	6.33

$0 \leq x \leq 1, 0 \leq t \leq 1$ , with parameters

$$\alpha_1 = 1, \quad \alpha_2 = 0, \quad k_1 = 10^6, \quad k_2 = 2k_1, \quad s_1 = 0, \quad s_2 = 1,$$

and with initial and boundary values

$$u(x, 0) = 1 + s_2x, \quad v(x, 0) = \frac{k_1}{k_2}u(x, 0) + \frac{s_2}{k_2}, \quad 0 \leq x \leq 1,$$

$$u(0, t) = \gamma_1(t), \quad v(0, t) = \gamma_2(t), \quad 0 \leq t \leq 1.$$

**Table 6**  $L_1$ -norm of errors versus stepsize for IMEX-GLM1, IMEX-GLM2, IMEX-GLM3, and IMEX-GLM4 applied to the discretization of (9.2) by first-order spatial discretization with  $N = 100$  points

$h$	1.00e-02	5.00e-03	2.50e-03	1.25e-03
IMEX-GLM1	4.19e-11	7.60e-12	1.61e-12	8.63e-13
IMEX-GLM2	5.15e-11	9.55e-12	2.76e-12	3.52e-13
IMEX-GLM3	3.80e-10	1.41e-10	6.38e-11	2.84e-11
IMEX-GLM4	*	2.92e-09	1.45e-09	6.56e-10

The entry \* indicates no convergence

(Observe that the condition  $v(0, t) = \gamma_2(t)$  does not have to be specified since  $\alpha_2 = 0$ ). Discretization of (9.2) in space variable  $x$  on the uniform grid  $x_i = i \Delta x, i = 0, 1, \dots, N, N \Delta x = 1$ , leads to the initial value problem for the system of ODEs of dimension  $2N$ , with non-stiff part corresponding to the advection terms, and stiff part corresponding to the reaction terms.

As in [29] we consider two discretizations of (9.2). The first one is based on the first-order upwind spatial discretization

$$\Delta x w'(x_i) = w(x_i) - w(x_{i-1}) + O(\Delta x^2), \quad i = 1, 2, \dots, N.$$

Assuming that  $\gamma_1(t) \equiv 1, 0 \leq t \leq 1$ , the initial values provide a stationary solution to the problem (9.2) and its discretization, compare [29]. The resulting system of ODEs was solved by IMEX GLMs (8.4), (8.8), (8.12), and (8.16) of order  $p = 1, 2, 3, 4$ , and the numerical results are presented in Table 6. These methods are referred to as IMEX-GLM1, IMEX-GLM2, IMEX-GLM3, and IMEX-GLM4.

The second discretization of (9.2) corresponds to the time dependent Dirichlet data  $\gamma_1(t) = 1 - \sin(12t)^4$  at the left boundary, and it is based on the fourth-order central differences in the interior domain

$$\Delta x w'(x_i) = \frac{1}{12} w(x_{i-2}) - \frac{2}{3} w(x_{i-1}) + \frac{2}{3} w(x_{i+1}) - \frac{1}{12} w(x_{i+2}) + O(\Delta x^5),$$

$i = 2, 3, \dots, N - 2$ , third-order finite differences

$$\Delta x w'(x_i) = -\frac{1}{3} w(x_{i-1}) - \frac{1}{2} w(x_i) + w(x_{i+1}) - \frac{1}{6} w(x_{i+2}) + O(\Delta x^4),$$

$$\Delta x w'(x_i) = \frac{1}{6} w(x_{i-2}) - w(x_{i-1}) + \frac{1}{2} w(x_i) + \frac{1}{3} w(x_{i+1}) + O(\Delta x^4),$$

at  $i = 1$  and  $i = N - 1$ , respectively, and on the one-sided finite difference of the third-order

$$\Delta x w'(x_i) = -\frac{1}{3} w(x_{i-3}) + \frac{3}{2} w(x_{i-2}) - 3w(x_{i-1}) + \frac{11}{6} w(x_i) + O(\Delta x^4),$$

at the right boundary point corresponding to  $i = N$ .

The solution to the resulting system of ODEs is smooth. This solution is plotted on Fig. 21, where the plot on the left corresponds to the approximation to the  $u(x, t)$  component and plot on the right corresponds to the approximation to the  $v(x, t)$  component of the solution to (9.2). The selection of numerical results is presented in Table 7 for the discretization of (9.2) with  $N = 400$  spatial points, where  $u_x$  and  $v_x$  are approximated by fourth-order central differences in the interior domain and by third-order finite differences at the boundaries as described above. The required starting values and the reference solution was computed by

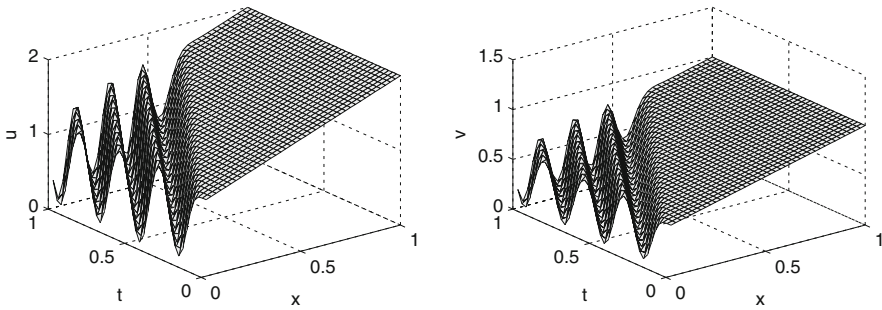


**Fig. 21** The approximation to the solution  $u(x, t)$  (left) and  $v(x, t)$  (right) of the discretization of (9.2) with  $N = 400$  spatial points, where  $u_x$  and  $v_x$  are approximated by fourth-order central differences in the interior domain and by third-order finite differences at the boundaries

**Table 7**  $L_1$ -norm of errors and observed orders of convergence  $p$  for IMEX GLMs with IRKS (8.4), (8.8), (8.12), and (8.16) applied to the discretization of (9.2) with  $N = 400$  by fourth-order central differences in the interior domain and by third-order finite differences at the boundaries

$h$	IMEX-GLM1		IMEX-GLM2		IMEX-GLM3		IMEX-GLM4	
	$\ error\ _1$	$p$	$\ error\ _1$	$p$	$\ error\ _1$	$p$	$\ error\ _1$	$p$
1.0000e-03			4.94e-01		8.14e-03		3.50e-04	
5.0000e-04			1.23e-01	2.00	1.02e-03	3.00	2.16e-05	4.02
2.5000e-04			3.08e-02	2.00	1.27e-04	3.00	1.35e-06	4.00
1.2500e-04	2.56e00		7.71e-03	2.00	1.59e-05	3.00	8.61e-08	3.97
6.2500e-05	1.27e00	1.02	1.93e-03	2.00	1.97e-06	3.01	2.51e-08	1.78
3.1250e-05	6.29e-01	1.01	4.82e-04	2.00	2.35e-07	3.07	2.47e-08	0.02
1.5625e-05	3.14e-01	1.00	1.20e-04	2.00	2.65e-08	3.15		
7.8125e-06	1.57e-01	1.00	3.01e-05	2.00				

ode15s with AbsTol =  $10^{-14}$  and RelTol =  $10^{-12}$ . In this table we have listed  $L_1$ -norm of the errors at the end of the interval of integration and the observed orders of convergence for IMEX GLMs (8.4), (8.8), (8.12), and (8.16) of order  $p = 1, 2, 3,$  and  $4$ . We can see that all these methods achieve the expected order of convergence and that there is no order reduction for this stiff system of ODEs. For this problem the ‘limiting accuracy’ is about  $10^{-8}$  and we can see that IMEX-GLM4 does not show significant improvement in accuracy consistent with order  $p = 4$  for stepsizes  $h < 1.25 \cdot 10^{-4}$ . The numerical results for other methods listed in Sect. 8 are similar to those presented in Table 7.

Our next example is the CUSP problem from [27] which is often used to test codes for stiff differential systems. This is a combination of Zeeman’s cusp catastrophe model for the nerve impulse mechanism [48] and the classical van der Pol oscillator. This problem is described by the system of PDEs of the form

$$\begin{cases} \frac{\partial y}{\partial t} = -\frac{1}{\epsilon} (y^3 + ay + b) \sigma \frac{\partial^2 y}{\partial x^2}, \\ \frac{\partial a}{\partial t} = b + 0.07 v + \sigma \frac{\partial^2 a}{\partial x^2}, \\ \frac{\partial b}{\partial t} = (1 - a^2) b - a - 0.4 y + 0.035 v + \sigma \frac{\partial^2 b}{\partial x^2}, \end{cases} \tag{9.3}$$

$0 \leq x \leq 1, t \in [0, t_{end}]$ , where  $v = u/(u + 0.1), u = (y - 0.7)(y - 1.3)$ . As in [27] we choose  $\sigma = 1/144$  and  $\epsilon = 10^{-4}$ . We discretize this problem by the method of lines on the uniform grid  $x_i = i \Delta x, i = 1, 2, \dots, N, N \Delta x = 1$ , which leads to the large system of ODEs of the form

$$\begin{cases} y'_i = -\frac{1}{\epsilon} (y_i^3 + a_i y_i + b_i) + \frac{\sigma}{\Delta x^2} (y_{i+1} - 2y_i + y_{i-1}), \\ a'_i = b_i + 0.07 v_i + \frac{\sigma}{\Delta x^2} (a_{i+1} - 2a_i + a_{i-1}), \\ b'_i = (1 - a_i^2)b_i - a_i - 0.4 y_i + 0.035 v_i + \frac{\sigma}{\Delta x^2} (b_{i+1} - 2b_i + b_{i-1}), \end{cases} \tag{9.4}$$

$i = 1, 2, \dots, N$ , where  $v_i = u_i/(u_i + 0.1), u_i = (y_i - 0.7)(y_i - 1.3)$ , and

$$y_i = y_i(t) \approx y(x_i, t), \quad a_i = a_i(t) \approx a(x_i, t), \quad b_i = b_i(t) \approx b(x_i, t).$$

We assume periodic boundary conditions

$$y_0 := y_N, \quad a_0 := a_N, \quad b_0 := b_N, \quad y_{N+1} := y_1, \quad a_{N+1} := a_1, \quad b_{N+1} := b_1,$$

and the initial conditions

$$y_i(0) = 0, \quad a_i(0) = -2 \sin\left(\frac{2i\pi}{N}\right), \quad b_i(0) = 2 \sin\left(\frac{2i\pi}{N}\right), \quad i = 1, 2, \dots, N.$$

We also choose  $N = 32$  and  $t_{end} = 1.1$ . The stiffness in this problem comes from a small parameter  $\epsilon$  and the discretization of the diffusion terms  $\partial^2 y/\partial x^2, \partial^2 a/\partial x^2$ , and  $\partial^2 b/\partial x^2$ , by central finite differences of the second order. In the IMEX schemes we treat the stiff terms in (9.4) by the implicit method and the remaining terms by the explicit method.

The solution to (9.4) is plotted in Fig. 22 in the coordinate system  $(y, a, b)$ , where we denoted by small black balls the beginnings and by small black squares the endings of the trajectories  $(y_i(t), a_i(t), b_i(t)), i = 1, 2, \dots, N$ . We can see that these trajectories are

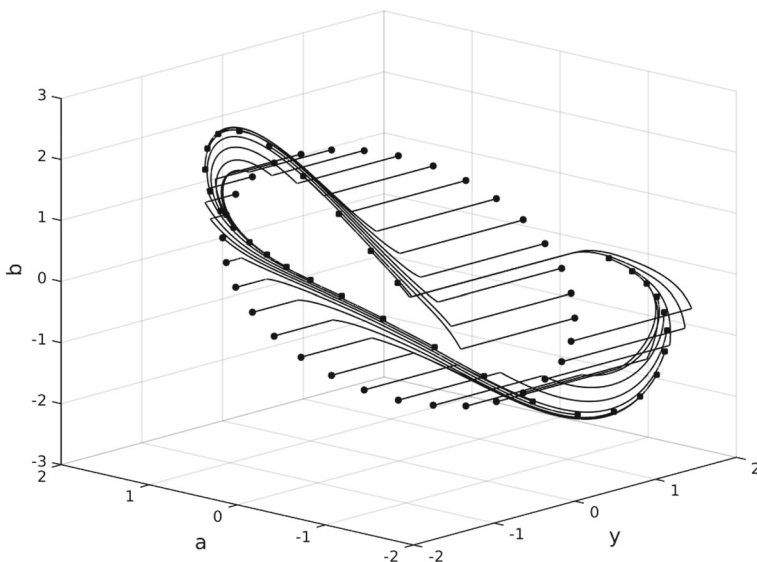


**Fig. 22** The approximation to the solutions  $(y_i(t), a_i(t), b_i(t))$  of the CUSP problem (9.4) for  $i = 1, 2, \dots, N, N = 32$ , and  $t \in [0, 1.1]$



**Table 8**  $L_1$ -norm of errors and observed orders of convergence  $p$  for IMEX GLMs with IRKS (8.4), (8.8), (8.12), and (8.16) applied to the discretization (9.4) of the CUSP problem (9.3) with  $N = 32$  by second-order central differences

$h$	IMEX-GLM1		IMEX-GLM2		IMEX-GLM3		IMEX-GLM4	
	$\ error\ _1$	$p$	$\ error\ _1$	$p$	$\ error\ _1$	$p$	$\ error\ _1$	$p$
1.0000e-04	4.96e-03		5.09e-04		1.43e-03			
5.0000e-05	2.51e-03	0.99	1.29e-04	1.98	2.50e-04	2.51		
2.5000e-05	1.26e-03	0.99	6.34e-05	1.03	1.00e-04	1.32	1.60e-03	
1.2500e-05	6.25e-04	1.01	1.52e-05	2.06	1.80e-05	2.48	1.56e-04	3.35
6.2500e-06	3.12e-04	1.00	1.97e-06	2.95	9.02e-07	4.32	4.15e-06	5.23
3.1250e-06	1.56e-04	1.00	4.98e-07	1.99	1.13e-08	6.32	3.12e-08	7.06
1.5625e-06	7.81e-05	1.00	1.25e-07	2.00	2.65e-10	5.41	7.31e-10	5.41

changing rapidly for some values of the parameter  $t$  and the use of rather small stepsizes  $h$  was necessary to resolve accurately these rapid changes. The results of numerical experiments for this problem are presented in Table 8 for time stepsizes  $h$  ranging from  $1.0 \cdot 10^{-4}$  to  $1.5625 \cdot 10^{-6}$ . We can see again that all IMEX schemes attain the expected order of convergence and there is no order reduction for any of these methods.

Following Hundsdorfer and Ruuth [28] (see also [29]) we consider next the adsorption–desorption problem given by the equations

$$\begin{cases} u_t + a(t)u_x = \kappa (v - \phi(u)), \\ v_t = -\kappa (v - \phi(u)), \end{cases} \tag{9.5}$$

$0 \leq x \leq 1, t \in [0, t_{end}]$ ,  $t_{end} = 1.25$ , where  $\phi(u) = k_1u/(1 + k_2u)$ . The initial values are  $u(x, 0) = v(x, 0) = 0, 0 \leq x \leq 1$ , and the boundary values are

$$\begin{cases} u(0, t) = 1 - \cos^2(6\pi t) & \text{if } a > 0. \\ u(1, t) = 0 & \text{if } a < 0. \end{cases}$$

As in [28] we choose the parameters  $\kappa = 10^6, k_1 = 50, k_2 = 100$ , and the velocity  $a = a(t) = -\arctan(100(t - 1))/\pi$ . Then  $a(t) > 0$  for  $0 \leq t \leq 1$ , which corresponds to the adsorption phase, and  $a(t) < 0$  for  $t > 1$ , which corresponds to the desorption phase.

For the spatial discretization of  $u_x$  we have implemented the WENO5 scheme [44] following the presentation in [45]. Using the method of lines approach on the uniform grid  $x_i = i\Delta x, i = 0, 1, \dots, N, N\Delta x = 1$ , we discretize  $u_t = -a(t)u_x$  by

$$u'_i = -\frac{1}{\Delta x} (\widehat{f}_{i+\frac{1}{2}} - \widehat{f}_{i-\frac{1}{2}}),$$

where  $\widehat{f}_{i+\frac{1}{2}}$  is the numerical flux, which for our problem is just equal to  $\widehat{f}(u) = f(u) = a(t)u$ . As in [45] we consider the Lax–Friedrichs splitting  $f(u) = f^+(u) + f^-(u)$ , where

$$f^+(u) = \frac{1}{2} (f(u) + mu), \quad f^-(u) = \frac{1}{2} (f(u) - mu),$$

and  $m = \max |f(u)|$ . This leads to  $f^+(u) = f(u)$  and  $f^-(u) = 0$ . We calculate next the indicators of smoothness

$$\begin{aligned} IS_0 &= \frac{13}{12}a^2 (u_{i-2} - 2u_{i-1} + u_i)^2 + \frac{1}{4}a^2 (u_{i-2} - 4u_{i-1} + 3u_i)^2, \\ IS_1 &= \frac{13}{12}a^2 (u_{i-1} - 2u_i + u_{i+1})^2 + \frac{1}{4}a^2 (u_{i-1} - u_{i+1})^2, \\ IS_2 &= \frac{13}{12}a^2 (u_i - 2u_{i+1} + u_{i+2})^2 + \frac{1}{4}a^2 (3u_i - 4u_{i+1} + u_{i+2})^2, \end{aligned}$$

and the non normalized stencil weights

$$\alpha_0 = \frac{1}{10} \left( \frac{1}{\epsilon + IS_0} \right)^2, \quad \alpha_1 = \frac{3}{5} \left( \frac{1}{\epsilon + IS_1} \right)^2, \quad \alpha_2 = \frac{3}{10} \left( \frac{1}{\epsilon + IS_2} \right)^2,$$

where  $\epsilon$  is a small positive number which is chosen, following the recommendation in [28], as  $\epsilon = 10^{-12}$ . We compute next the normalized WENO stencil weights from the relations

$$w_0 = \frac{\alpha_0}{\alpha_0 + \alpha_1 + \alpha_2}, \quad w_1 = \frac{\alpha_1}{\alpha_0 + \alpha_1 + \alpha_2}, \quad w_2 = \frac{\alpha_2}{\alpha_0 + \alpha_1 + \alpha_2}.$$

The numerical fluxes for WENO5 scheme are then given by

$$\begin{aligned} \widehat{f}_{i+\frac{1}{2}} &= w_0 a \left( \frac{1}{3}u_{i-2} - \frac{7}{6}u_{i-1} + \frac{11}{6}u_i \right) + w_1 a \left( -\frac{1}{6}u_{i-1} + \frac{5}{6}u_i + \frac{1}{3}u_{i+1} \right) \\ &+ w_2 a \left( \frac{1}{3}u_i + \frac{5}{6}u_{i+1} - \frac{1}{6}u_{i+2} \right). \end{aligned}$$

The discretization of (9.5) is then given by the following system of ODEs

$$\begin{cases} u'_i = -\frac{1}{\Delta x} \left( \widehat{f}_{i+\frac{1}{2}} - \widehat{f}_{i-\frac{1}{2}} \right) + \kappa (v_i - \phi(u_i)), \\ v'_i = -\kappa (v_i - \phi(u_i)), \end{cases} \tag{9.6}$$

$i = 1, 2, \dots, N, t \in [0, 1]$ , where  $u_0 = 1 - \cos^2(6\pi t)$ . The initial conditions are  $u_i(0) = v_i(0) = 0, i = 1, 2, \dots, N$ . This system has to be modified for  $t \geq 1$ , where we consider the discretization of the problem (9.5) by the method of lines on the spatial grid  $x_i = (i - 1)\Delta x, i = 1, 2, \dots, N, N\Delta x = 1$ , and assume that  $u_{N+1} = 0$ , which corresponds to the boundary condition  $u(1, t) = 0$ . This condition has to be taken into account for  $t \geq 1$  when the velocity  $a(t)$  becomes negative.

We have plotted on Fig. 23 the approximations to  $u_i(t) \approx u(x_i, t)$  and  $v_i(t) \approx v(x_i, t)$  corresponding to  $N = 800$  and  $i = 200$ . We can see that these trajectories are changing rapidly (there are smooth regions between the shocks) and we had to use quite small stepsizes to resolve them accurately. The selection of numerical results is presented in Table 9 for stepsizes  $h$  ranging from  $2.5000 \cdot 10^{-4}$  to  $7.8125 \cdot 10^{-6}$ . In this table the error is defined by

$$\text{error} = \begin{bmatrix} y(x_1, t_{end}) - y_1(t_{end}) \\ \vdots \\ y(x_N, t_{end}) - y_N(t_{end}) \end{bmatrix}, \quad y(x, t) = \begin{bmatrix} u(x, t) \\ v(x, t) \end{bmatrix}, \quad y_i(t) = \begin{bmatrix} u_i(t) \\ v_i(t) \end{bmatrix},$$

where  $y = [u, v]^T$  is the solution to (9.5). The approximation to this reference solution was computed using `ode15s` from Matlab with  $\text{AbsTol} = 10^{-14}$  and  $\text{RelTol} = 10^{-12}$ . These results demonstrate again that all methods achieve the expected order of accuracy and do not exhibit the order reduction phenomenon.

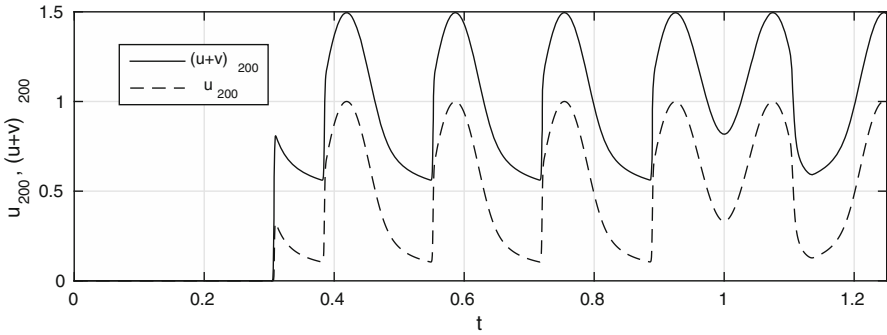


**Fig. 23** Approximations to the trajectories  $u_{200}(t)$  and  $(u+v)_{200}(t)$  of the discretization (9.6) of the problem (9.5) with  $N = 800$  spatial points, where  $u_x$  is approximated by WENO5 scheme

Following [29] our next test model for the IMEX schemes is the system of reaction–diffusion equations

$$\begin{cases} \frac{\partial u}{\partial t} = D_1 \left( \frac{\partial^2 u}{\partial x^2} + \frac{\partial^2 u}{\partial y^2} \right) + \kappa (a - u + u^2 v), \\ \frac{\partial v}{\partial t} = D_2 \left( \frac{\partial^2 v}{\partial x^2} + \frac{\partial^2 v}{\partial y^2} \right) + \kappa (b - u^2 v), \end{cases} \tag{9.7}$$

$0 \leq x, y \leq 1, t \geq 0$ , with initial conditions

$$\begin{aligned} u(x, y, 0) &= a + b + 10^{-3} \exp \left( -100 \left( \left( x - \frac{1}{2} \right)^2 + \left( y - \frac{1}{3} \right)^2 \right) \right), \\ v(x, y, 0) &= \frac{b}{(a + b)^2}, \end{aligned}$$

and the homogeneous Neumann boundary conditions

$$\begin{aligned} \frac{\partial u}{\partial x}(0, y, t) = \frac{\partial u}{\partial x}(1, y, t) = 0, \quad \frac{\partial u}{\partial y}(x, 0, t) = \frac{\partial u}{\partial y}(x, 1, t) = 0, \\ \frac{\partial v}{\partial x}(0, y, t) = \frac{\partial v}{\partial x}(1, y, t) = 0, \quad \frac{\partial v}{\partial y}(x, 0, t) = \frac{\partial v}{\partial y}(x, 1, t) = 0. \end{aligned}$$

The parameter values are  $a = 0.1305, b = 0.7695, D_1 = 0.05, D_2 = 1, \kappa = 100$ . This model is due to Schnackenberg [43] and, as observed in [29], it is related to the Gray-Scott model for pattern formation described in [40].

The system (9.7) was discretized on the uniform grids in space variables  $x$  and  $y, x_i = (i - 1)\Delta x, i = 1, 2, \dots, N, (N - 1)\Delta x = 1, y_j = (j - 1)\Delta y, j = 1, 2, \dots, M, (M - 1)\Delta y = 1$ , using standard second order finite differences in space for the diffusion terms. This leads to the system of ODEs of dimension  $2NM$  for the unknown functions  $u_{ij}(t) \approx u(x_i, y_j, t)$  and  $v_{ij}(t) \approx v(x_i, y_j, t)$  of the form

$$\begin{cases} u'_{ij} = D_1 \left( \frac{u_{i+1,j} - 2u_{ij} + u_{i-1,j}}{\Delta x^2} + \frac{u_{i,j+1} - 2u_{ij} + u_{i-1,j}}{\Delta y^2} \right) \\ \quad - u_{ij} v_{ij}^2 + \gamma (1 - u_{ij}), \\ v'_{ij} = D_2 \left( \frac{v_{i+1,j} - 2v_{ij} + v_{i-1,j}}{\Delta x^2} + \frac{v_{i,j+1} - 2v_{ij} + v_{i-1,j}}{\Delta y^2} \right) \\ \quad + u_{ij} v_{ij}^2 - (\gamma + \kappa) v_{ij}, \end{cases} \tag{9.8}$$

**Table 9**  $L_1$ -norm of errors and observed orders of convergence  $p$  for IMEX GLMs with IRKS (8.4), (8.8), (8.12), and (8.16) applied to the discretization (9.6) of the adsorption–desorption Eq. (9.5) with  $N = 800$  spatial points by WENO5 scheme

$h$	IMEX-GLM1		IMEX-GLM2		IMEX-GLM3		IMEX-GLM4	
	$\ error\ _1$	$p$	$\ error\ _1$	$p$	$\ error\ _1$	$p$	$\ error\ _1$	$p$
2.5000e-04	1.33e01		5.94e-01		3.98e-02			
1.2500e-04	7.21e00	0.88	1.48e-01	2.00	4.07e-03	3.29	8.62e-04	
6.2500e-05	4.56e00	0.66	3.68e-02	2.01	5.10e-04	3.00	6.11e-05	3.82
3.1250e-05	2.18e00	1.06	9.18e-03	2.00	6.36e-05	3.00	3.39e-06	4.17
1.5625e-05	1.01e00	1.11	2.29e-03	2.00	7.86e-06	3.02	4.20e-07	3.01
7.8125e-06	4.92e-01	1.04	5.73e-04	2.00	9.93e-07	2.98	3.62e-07	0.21

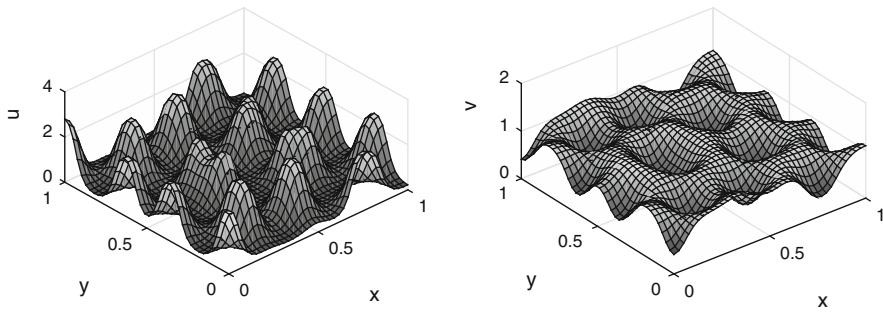


**Fig. 24** The approximation to the solution  $u(x, y, t)$  (left) and  $v(x, y, t)$  (right) of the discretization (9.8) of the system (9.7) by second order finite differences with  $N = M = 41$  spatial points in  $x$  and  $y$  variables

$i = 1, 2, \dots, N, j = 1, 2, \dots, M$ , with initial conditions

$$u_{ij}(0) = a + b + 10^{-3} \exp\left(-100\left(\left(x_i - \frac{1}{2}\right)^2 + \left(y_j - \frac{1}{3}\right)^2\right)\right),$$

$$v_{ij}(0) = \frac{b}{(a + b)^2},$$

$i = 1, 2, \dots, N, j = 1, 2, \dots, M$ . Because of the boundary conditions we have

$$u_{0,j} = u_{2,j}, \quad u_{N+1,j} = u_{N-1,j}, \quad u_{i,0} = u_{i,2}, \quad u_{i,M+1} = u_{i,M-1},$$

$$v_{0,j} = v_{2,j}, \quad v_{N+1,j} = v_{N-1,j}, \quad v_{i,0} = v_{i,2}, \quad v_{i,M+1} = v_{i,M-1}.$$

This system of ODEs (9.8) was then solved by IMEX schemes (8.4), (8.8), (8.12), and (8.16), where the diffusion terms were treated by implicit method and the reaction terms by the explicit methods. The reference solution at  $t = 1$  is plotted on Fig. 24, and the selection of the results of numerical experiments are presented in Table 10. We can see that the methods IMEX-GLM1, IMEX-GLM2, IMEX-GLM3, achieve the expected order of convergence, and the observed order of the method IMEX-GLM4 for small sizes is more than four, and that there is no order reduction for some range of stepsizes on the whole interval of integration.

The order reduction phenomenon for GLMs of order  $p$  and stage order  $q$  is discussed in a recent paper [9]. It was proved in this paper that if the GLM, whose region of absolute stability  $\mathcal{A}$  is closed in  $\overline{\mathbb{C}}$ , is applied to the Prothero–Robinson problem (6.9), then the global

**Table 10**  $L_1$ -norm of errors and observed orders of convergence  $p$  for IMEX GLMs with IRKS (8.4), (8.8), (8.12), and (8.16) applied to the discretization of reaction–diffusion Eq. (9.7) by second order finite differences in space variables for the diffusion terms

$h$	IMEX-GLM1		IMEX-GLM2		IMEX-GLM3		IMEX-GLM4	
	$\ \text{error}\ _1$	$p$	$\ \text{error}\ _1$	$p$	$\ \text{error}\ _1$	$p$	$\ \text{error}\ _1$	$p$
1.0000e−03	1.15e02		7.01e−01		1.38e−01		2.07e00	
5.0000e−04	5.59e01	1.04	1.94e−01	1.85	1.73e−02	3.00	5.80e−01	1.83
2.5000e−04	3.60e01	0.63	5.19e−02	1.90	2.11e−03	3.03	3.37e−02	4.11
1.2500e−04	1.09e01	1.72	1.35e−02	1.95	2.58e−04	3.03	1.32e−03	4.68
6.2500e−05	4.83e00	1.18	3.43e−03	1.97	3.19e−05	3.02	4.50e−05	4.87
3.1250e−05	2.37e00	1.03	8.66e−04	1.99	3.95e−06	3.01	1.48e−06	4.92

error  $e^{[n]}$  satisfies

$$\|e^{[n]}\| = O(h^q) + O(h^p) \text{ as } h \rightarrow 0 \text{ and } h\mu \rightarrow -\infty.$$

Moreover, if the GLM has RK stability and  $R(\infty) \neq 1$ , where  $R(z)$  is the stability function of the underlying RK method, then we have a better estimate

$$\|e^{[n]}\| = O(h^{q+1}) + O(h^p) \text{ as } h \rightarrow 0 \text{ and } h\mu \rightarrow -\infty.$$

In particular, there is no order reduction for GLMs with RK stability and such that  $R(\infty) \neq 1$  of order  $p$  and stage order  $q = p - 1$ , i.e., for such methods  $\|e^{[n]}\| = O(h^p)$  as  $h \rightarrow 0$  and  $h\mu \rightarrow -\infty$ .

### 10 Concluding Remarks

We described a construction of a new class of IMEX GLMs with IRKS. This construction starts with a highly stable diagonally implicit GLMs of order  $p$  and stage order  $q = p$ , and then we ‘remove’ the implicitness of the terms corresponding to the non-stiff part of the differential system by extrapolating stage derivatives in the current step by the stage derivatives in the previous step and those already computed in the current step. The new methods have order  $p$  and stage order  $q = p$  and, contrary to some classes of IMEX Runge–Kutta methods, they do not suffer from order reduction phenomenon. This is confirmed by numerical experiments on a wide range of nontrivial test problems from real life applications.

Future work will address the implementation issues related to these methods such as construction of appropriate starting and finishing procedures, estimation of local discretization errors, step size and order changing strategies, construction of continuous extensions, and efficient solution of nonlinear systems of equations corresponding to the stiff part of the method at each step of integration.

**Acknowledgements** The research reported in this paper was started during the visit of the first author (MB) to the Arizona State University in November 2014. This author wish to express his gratitude to the School of Mathematical and Statistical Sciences for hospitality during this visit.

## References

- Abdulle, A., Vilmart, G.: PIROCK: a swiss-knife partitioned implicit–explicit orthogonal Runge–Kutta–Chebyshev integrator for stiff diffusion–advection–reaction problems with or without noise. *J. Comput. Phys.* **242**, 869–888 (2013)
- Ascher, U.M., Ruuth, S.J., Spiteri, R.J.: Implicit–explicit Runge–Kutta methods for time-dependent partial differential equations. *Appl. Numer. Math.* **25**, 151–167 (1997)
- Ascher, U.M., Ruuth, S.J., Wetton, B.: Implicit–explicit methods for time dependent PDE’s. *SIAM J. Numer. Anal.* **32**, 797–823 (1995)
- Beck, S., Weiner, R., Podhaisky, H., Schmitt, B.A.: Implicit peer methods for large stiff ODE systems. *J. Appl. Math. Comput.* **38**, 389–406 (2012)
- Boscarino, S.: Error analysis of IMEX Runge–Kutta methods derived from differential–algebraic systems. *SIAM J. Numer. Anal.* **45**, 1600–1621 (2007)
- Boscarino, S.: On the accurate third order implicit–explicit Runge–Kutta methods for stiff problems. *Appl. Numer. Math.* **59**, 1515–1528.37 (2009), B305–B331 (2015)
- Ascher, U.M., Bürger, R., Mulet, P., Russo, G., Villada, M.L.: Linearly implicit IMEX Runge–Kutta methods for a class of degenerate convection–diffusion problems. *SIAM J. Sci. Comput.* **37**, B305–B331 (2015). doi:[10.1137/140967544](https://doi.org/10.1137/140967544)
- Boscarino, S., Russo, G.: On a class of uniformly accurate IMEX Runge–Kutta schemes and applications to hyperbolic systems with relaxation. *SIAM J. Sci. Comput.* **31**, 1926–1945 (2009)
- Braś, M., Cardone, A., Jackiewicz, Z., Welfert, B.: Order reduction phenomenon for general linear methods. *SIAM J. Numer. Anal.* (submitted)
- Butcher, J.C.: *The Numerical Analysis of Ordinary Differential Equations. Runge–Kutta and General Linear Methods*. Wiley, Chichester (1987)
- Butcher, J.C.: Diagonally-implicit multi-stage integration methods. *Appl. Numer. Math.* **11**, 347–363 (1993)
- Butcher, J.C.: *Numerical Methods for Ordinary Differential Equations*. Wiley, Chichester (2003)
- Butcher, J.C.: General linear methods. *Acta Numer.* **15**, 157–256 (2006)
- Butcher, J.C., Jackiewicz, Z.: Diagonally implicit general linear methods for ordinary differential equations. *BIT* **33**, 452–472 (1993)
- Butcher, J.C., Jackiewicz, Z.: Construction of general linear methods with Runge–Kutta stability properties. *Numer. Algorithms* **36**, 53–72 (2004)
- Butcher, J.C., Jackiewicz, Z., Wright, W.M.: Error propagation for general linear methods for ordinary differential equations. *J. Complex.* **23**, 560–580 (2007)
- Butcher, J.C., Wright, W.M.: The construction of practical general linear methods. *BIT* **43**, 695–721 (2003)
- Calvo, M.P., de Frutos, J., Novo, J.: Linearly implicit Runge–Kutta methods for advection–diffusion–reaction problems. *Appl. Numer. Math.* **37**, 535–549 (2001)
- Cardone, A., Jackiewicz, Z., Sandu, A., Zhang, H.: Extrapolation-based implicit–explicit general linear methods (2013), [arXiv:1304.2276](https://arxiv.org/abs/1304.2276)
- Cardone, A., Jackiewicz, Z., Sandu, A., Zhang, H.: Extrapolation-based implicit–explicit general linear methods. *Numer. Algorithms* **65**, 377–399 (2014)
- Cardone, A., Jackiewicz, Z., Sandu, A., Zhang, H.: Extrapolated implicit–explicit Runge–Kutta methods. *Math. Model. Anal.* **19**, 18–43 (2014)
- Cardone, A., Jackiewicz, Z., Sandu, A., Zhang, H.: Construction of highly stable implicit-explicit general linear methods. In: *Discrete and Continuous Dynamical Systems. Series S*, vol. 2015, pp. 185–194 (2015)
- Crouzeix, M.: Une méthode multipas implicite-explicite pour l’approximation des équations d’évolution paraboliques. *Numer. Math.* **35**, 257–276 (1980)
- Dym, H., McKean, H.P.: *Fourier Series and Integrals*. Academic Press, New York (1972)
- Frank, J., Hundsdorfer, W., Verwer, J.G.: On the stability of implicit–explicit linear multistep methods. *Appl. Numer. Math.* **25**, 193–205 (1997)
- Hairer, E., Nørsett, S.P., Wanner, G.: *Solving Ordinary Differential Equations I: Nonstiff Problems*. Springer, New York (1993)
- Hairer, E., Wanner, G.: *Solving Ordinary Differential Equations II. Stiff and Differential–Algebraic Problems*. Springer, Berlin (1996)
- Hundsdorfer, W., Ruuth, S.J.: IMEX extensions of linear multistep methods with general monotonicity and boundedness properties. *J. Comput. Phys.* **225**, 2016–2042 (2007)
- Hundsdorfer, W., Verwer, J.G.: *Numerical Solution of Time-Dependent Advection–Diffusion–Reaction Equations*. Springer, Berlin, Heidelberg, New York (2003)

30. Izzo, G., Jackiewicz, Z.: Highly stable implicit–explicit Runge–Kutta methods. *Appl. Numer. Math.* (submitted)
31. Jackiewicz, Z.: Implementation of DIMSIMs for stiff differential systems. *Appl. Numer. Math.* **42**, 251–267 (2002)
32. Jackiewicz, Z.: Construction and implementation of general linear methods for ordinary differential equations. A review. *J. Sci. Comput.* **25**, 29–49 (2005)
33. Jackiewicz, Z.: *General Linear Methods for Ordinary Differential Equations*. Wiley, Hoboken (2009)
34. Jebens, S., Knoth, O., Weiner, R.: Partially implicit peer methods for the compressible Euler equations. *J. Comput. Phys.* **230**, 4955–4974 (2011)
35. Kennedy, C.A., Carpenter, M.H.: Additive Runge–Kutta schemes for convection–diffusion–reaction equations. *Appl. Numer. Math.* **44**, 139–181 (2003)
36. Layton, A.T., Minion, M.L.: Implications of the choice of quadrature nodes for Picard integral deferred correction methods for ordinary differential equations. *BIT* **45**, 341–373 (2005)
37. Minion, M.L.: Semi-implicit projection methods for incompressible flow based on spectral deferred corrections. *Appl. Numer. Math.* **48**, 369–387 (2004)
38. Pareschi, L., Russo, G.: Implicit–explicit Runge–Kutta schemes for stiff systems of differential equations. *Recent trends in numerical analysis*, 269–288. *Adv. Theory Comput. Math.*, **3**, Nova Science Publishers, Huntington, NY (2001)
39. Pareschi, L., Russo, G.: Implicit–explicit Runge–Kutta schemes and applications to hyperbolic systems with relaxation. *J. Sci. Comput.* **25**, 129–155 (2005)
40. Pearson, J.E.: Complex patterns in a simple systems. *Science* **261**, 189–192 (1993)
41. Prothero, A., Robinson, A.: On the stability and accuracy of one-step methods for solving stiff systems of ordinary differential equations. *Math. Comput.* **28**, 145–162 (1974)
42. Shampine, L.F., Sommeijer, B.P., Verwer, J.G.: IRKC: an IMEX solver for stiff diffusion–reaction PDEs. *J. Comput. Appl. Math.* **196**, 485–497 (2006)
43. Schnakenberg, J.: Simple chemical reaction systems with limiting cycle behaviour. *J. Theor. Biol.* **81**, 389–400 (1979)
44. Shu, C.-W.: High order ENO and WENO schemes for computational fluid dynamics. In: Barth, T.J., Deconinck, H. (eds.) *High-Order Methods for Computational Physics*. Lecture Notes in Computational Science and Engineering, vol. 9, pp. 439–582. Springer, Berlin (1999)
45. Wang, R., Spiteri, R.J.: Linear instability of the fifth-order WENO method. *SIAM J. Numer. Anal.* **45**, 1871–1901 (2007)
46. Wright, W.: *General linear methods with inherent Runge–Kutta stability*, Ph.D. thesis, The University of Auckland, New Zealand (2002)
47. Wright, W.: Explicit general linear methods with inherent Runge–Kutta stability. *Numer. Algorithms* **31**, 381–399 (2002)
48. Zeeman, E.C.: *Differential Equations for the Heartbeat and Nerve Impulse*. In: Waddington, C.H. (ed.) *Towards a Theoretical Biology*, vol. 4, pp. 4–67. Edinburgh University Press, Edinburgh (1972)
49. Zhang, H., Sandu, A., Blaise, S.: High order implicit–explicit general linear methods with optimized stability regions (2014). [arXiv:1407.2337](https://arxiv.org/abs/1407.2337)
50. Zhang, H., Sandu, A., Blaise, S.: Partitioned and implicit–explicit general linear methods for ordinary differential equations. *J. Sci. Comput.* **61**, 119–144 (2014)
51. Zharovsky, E., Sandu, A., Zhang, H.: A class of implicit–explicit two-step Runge–Kutta methods. *SIAM J. Numer. Anal.* **53**, 321–341 (2015)